Oxide MBE—
A Tool to Create
Artificial Quantum Materials

Darrell G. Schlom

Department of Materials Science and Engineering
Cornell University

Kavli Institute at Cornell for Nanoscale Science

Outline

- What is MBE and what is it good for?
  Greatest hits of MBE

- How to grow your favorite oxide quantum material by MBE?
  Nuts and bolts of oxide MBE

- Oxide MBE growth of quantum materials
  Case studies—including Sr_2RuO_4

- How can I gain access to an oxide MBE if I don’t have one?
  Use PARADIM’s oxide MBE (+ ARPES + …)

MBE ≈ Atomic Spray Painting

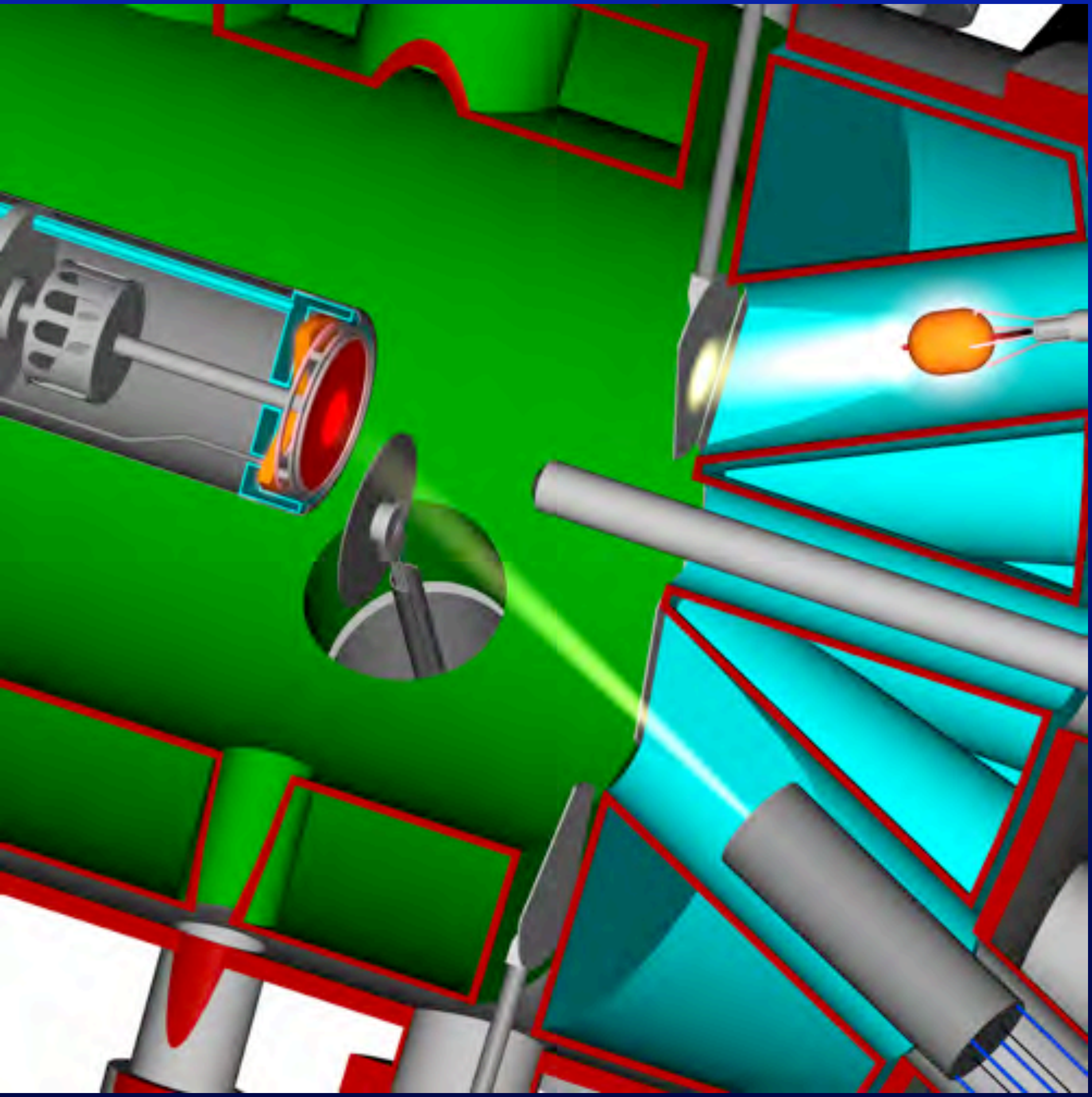

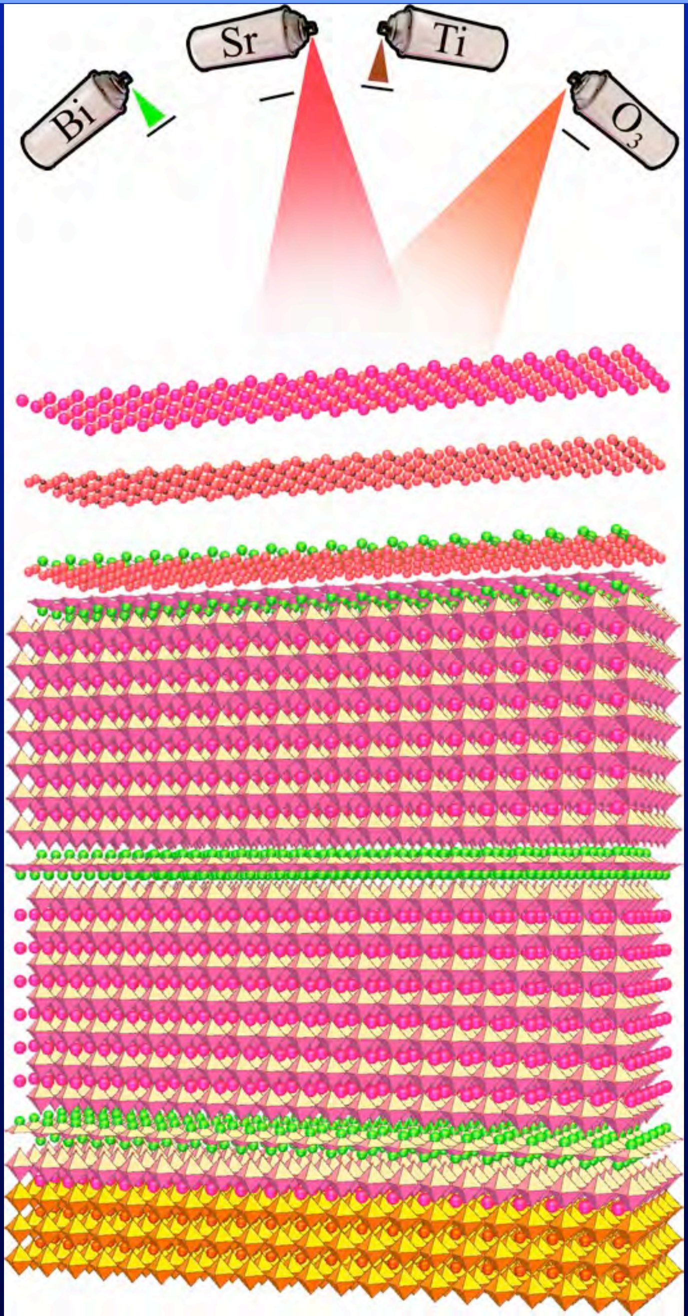

When GaAs is Heated …

J. Phys. Chem. Solids Pergamon Press 1967. Vol. 28, pp. 2257–2267. Printed in Great Britain.

VAPOR PRESSURES AND PHASE EQUILIBRIA IN THE Ga–As SYSTEM

J. R. ARTHUR

Bell Telephone Laboratories, Incorporated, Murray Hill, New Jersey

(*Received* 9 *March* 1967; *in revised form* 18 *May* 1967)

Abstract—Mass spectrometric and weight loss measurements of the species effusing from a Knudsen cell containing GaAs were used to obtain vapor pressures over the temperature range 900–1200°K. The As_2/As_4 ratio was observed in these measurements to be substantially larger than previously reported[2,3] when precautions were taken to prevent the buildup of arsenic vapor in the mass spectrometer ionization chamber. A third law treatment of the data gave enthalpies for the reactions:

$$GaAs_{(s)} \rightarrow Ga_{(s)} + \tfrac{1}{2}As_{2(g)} \qquad \Delta H_{298}{}^0 = 44{\cdot}9 \text{ kcal}$$
$$GaAs_{(s)} \rightarrow Ga_{(s)} + \tfrac{1}{4}As_{4(g)} \qquad \Delta H_{298}{}^0 = 29{\cdot}4 \text{ kcal}$$
$$2As_{2(g)} \rightarrow As_{4(g)} \qquad \Delta H_{298}{}^0 = -62{\cdot}5 \text{ kcal}$$
$$GaAs_{(s)} \rightarrow Ga_{(g)} + As_{(g)} \qquad \Delta H_{298}{}^0 = 155 \text{ kcal}$$

These results were used to correct Thurmond's calculations of vapor pressures and activity coefficients along the GaAs liquidus.[1]

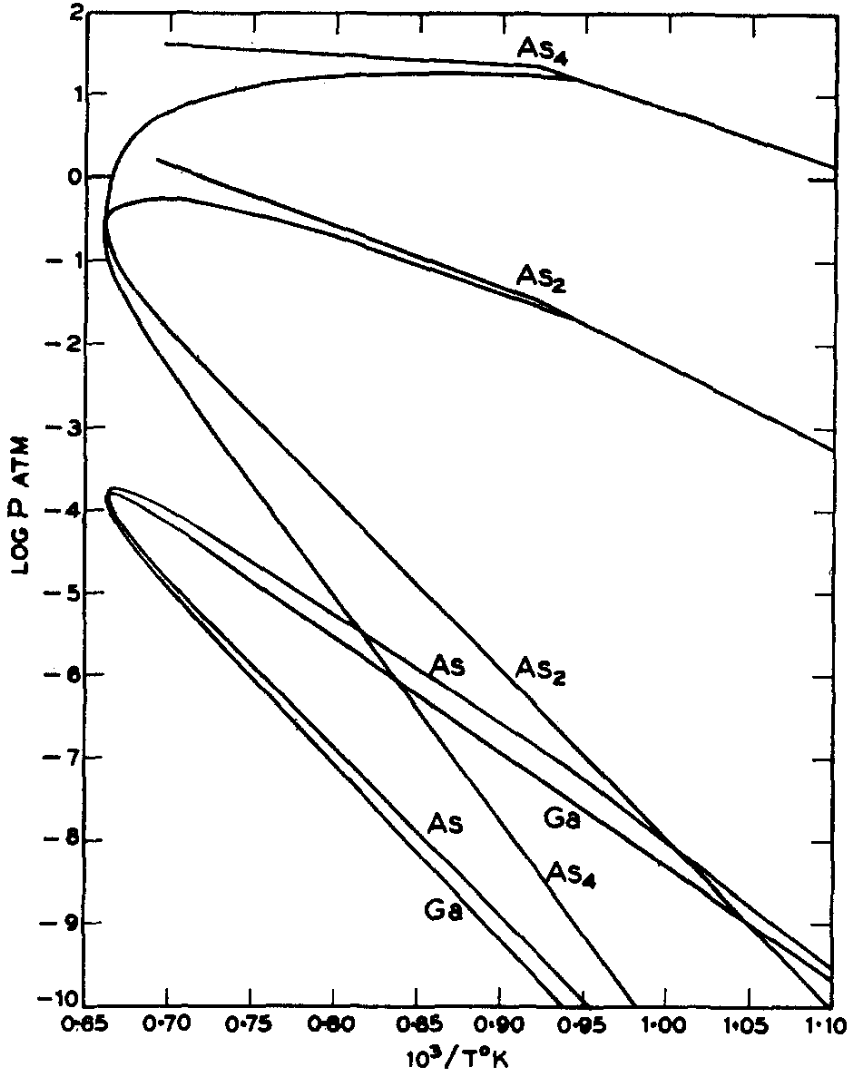

FIG. 5. Equilibrium vapor pressures of As, As_2, As_4 and Ga along the binary liquidus as a function of T^{-1}. Pressures of As_2 and As_4 over pure solid and liquid As are also shown.

Consider Evaporation of PbO

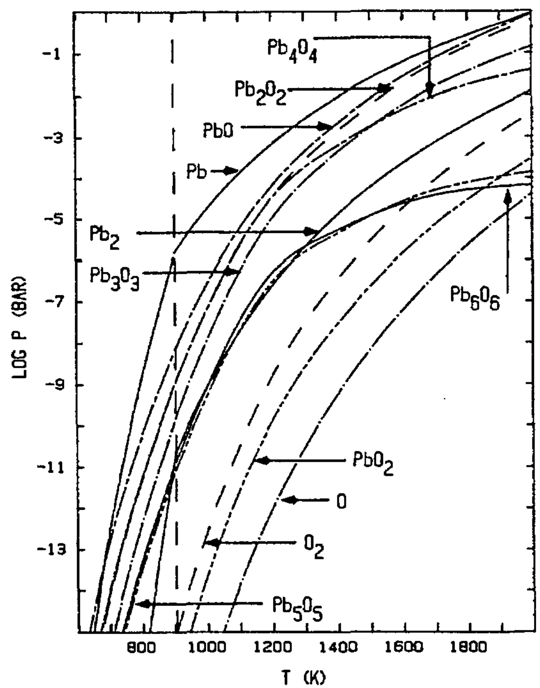

FIG. 53. PbO vaporization in 10^{-15} bar O_2 below 905 K and vaporization of Pb–PbO mixture above 905 K.

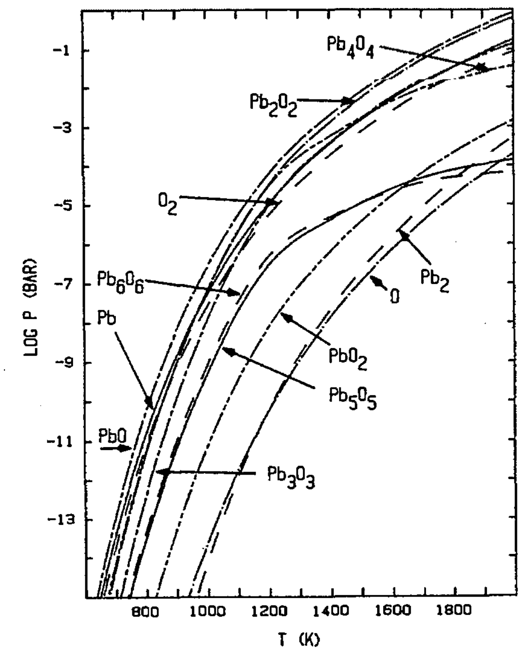

FIG. 54. PbO congruent vaporization.

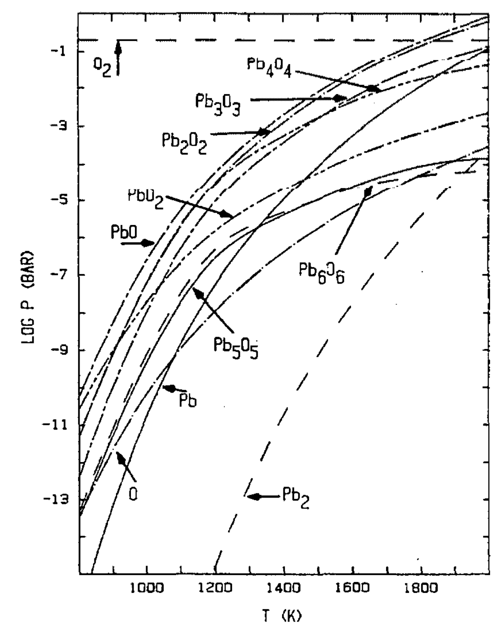

FIG. 55. PbO vaporization in 0.2 bar O_2.

R.H. Lamoreaux and D.L. Hildenbrand,
"High-Temperature Vaporization Behavior of Oxides II. Oxides of Be, Mg, Ca, Sr, Ba, B, Al, Ga, In, Tl, Si, Ge, Sn, Pb, Zn, Cd, and Hg,"
J. Phys. Chem. Ref. Data **16** (1987) 419-443.

Key Enablers of MBE

- “3-Temperaturaufdampfverfahren” for Growth of III-V Semiconductor Films by Vacuum Evaporation
  K.G. Günther, “Aufdampfschichten aus halbleitenden III-V Verbindungen,” *Zeitschrift für Naturforschung A* **13** (1958) 1081-1089.

- Reliable UHV Sealing Technology
  W.R. Wheeler and M. Carlson, “Ultra-High Vacuum Flanges,” *Transactions of the Eighth National Vacuum Symposium*, edited by L.E. Preuss (Pergamon, New York, 1962), pp. 1309-1318.
  M.A. Carlson and W.R. Wheeler, “Metal Vacuum Joint,” U.S. Patent #3,208,758 (Sept. 28, 1965).

Epitaxial GaAs by 3-Temperature-Technique

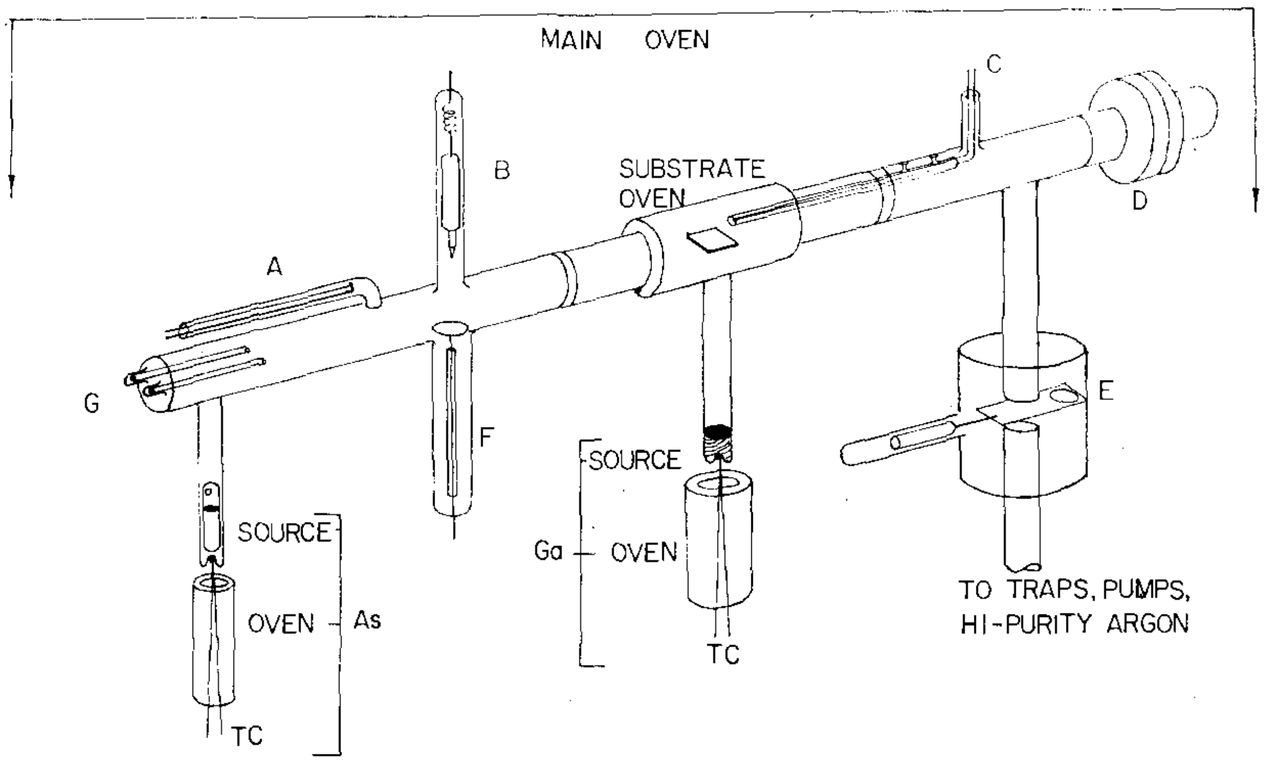

FIG. 1. GaAs film evaporation system: (A) Pirani gauge; (B) electrical contact to diode structure; (C) thermocouple; (D) metal flanges and viton gaskets as an entrance port for loading system; (E) particulate valve; (F) circular Ta plate; positive electrode in diode structure; (G) quartz rods which extend the length of the envelope and which guide the substrate carrier.

J.E. Davey and T. Pankey, "Epitaxial GaAs Films Deposited by Vacuum Evaporation," *Journal of Applied Physics* **39** (1968) 1941-1948.

UHV Seals—Varian Conflat®

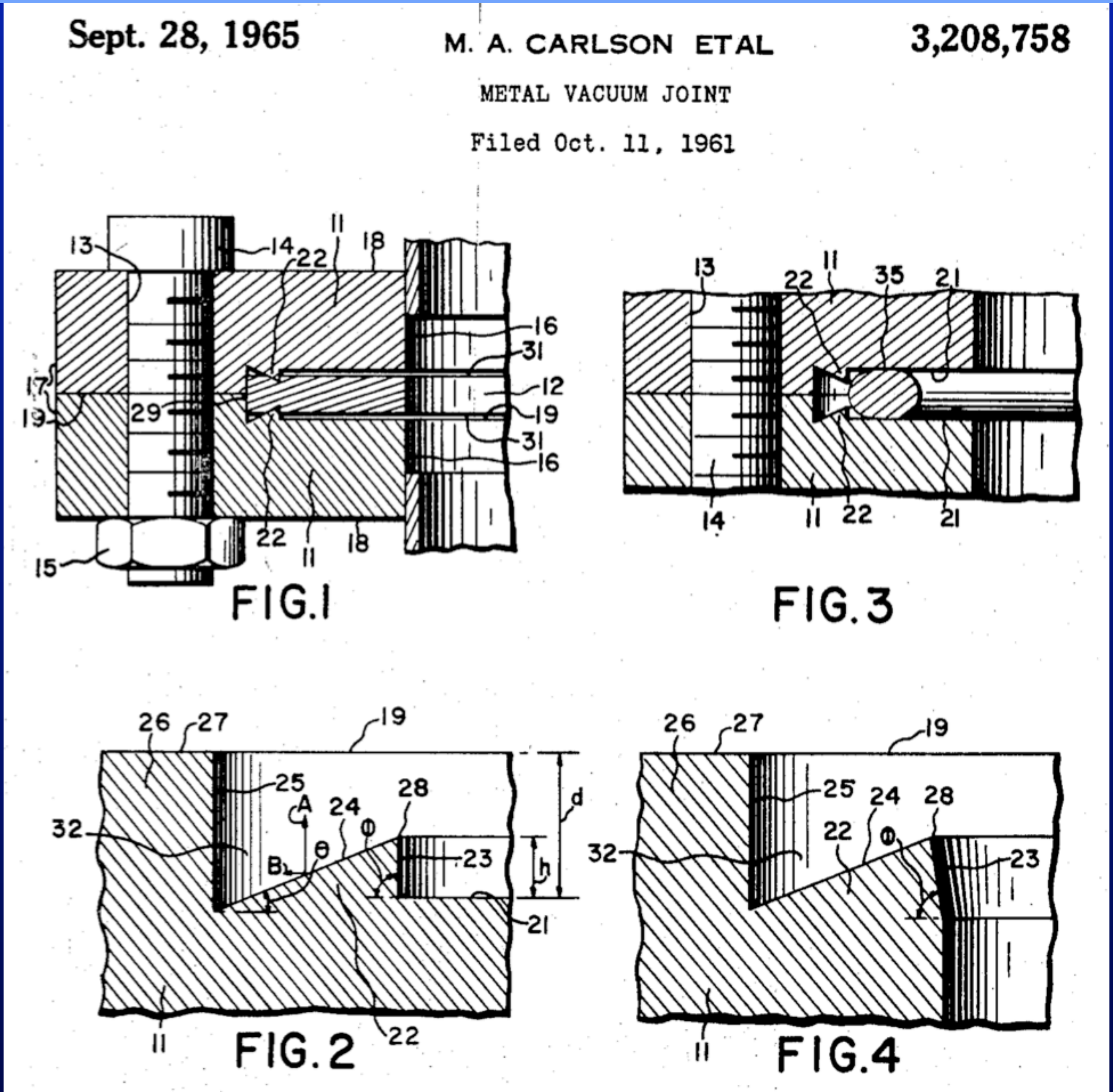

M.A. Carlson and W.R. Wheeler, "Metal Vacuum Joint," U.S. Patent #3,208,758 (Sept. 28, 1965)

Evolution of MBE

1st MBE
Al Cho at Bell Labs, 1972

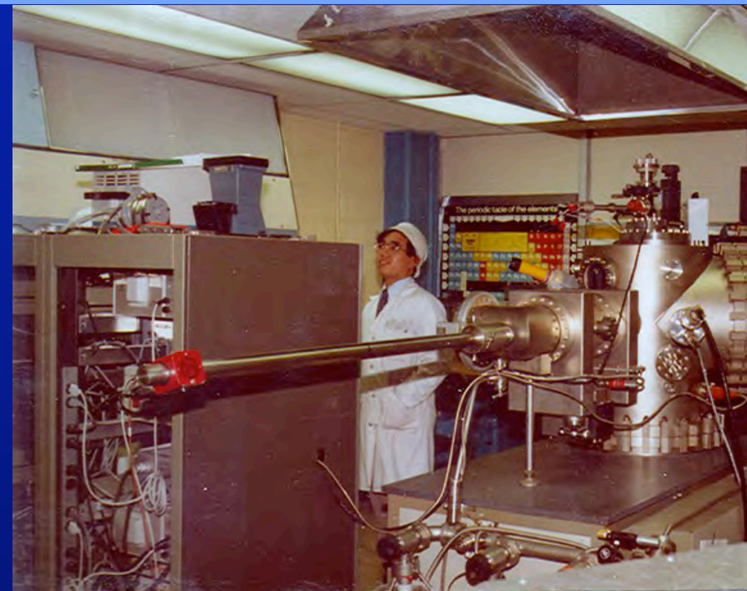

1st University MBE Cornell, 1978

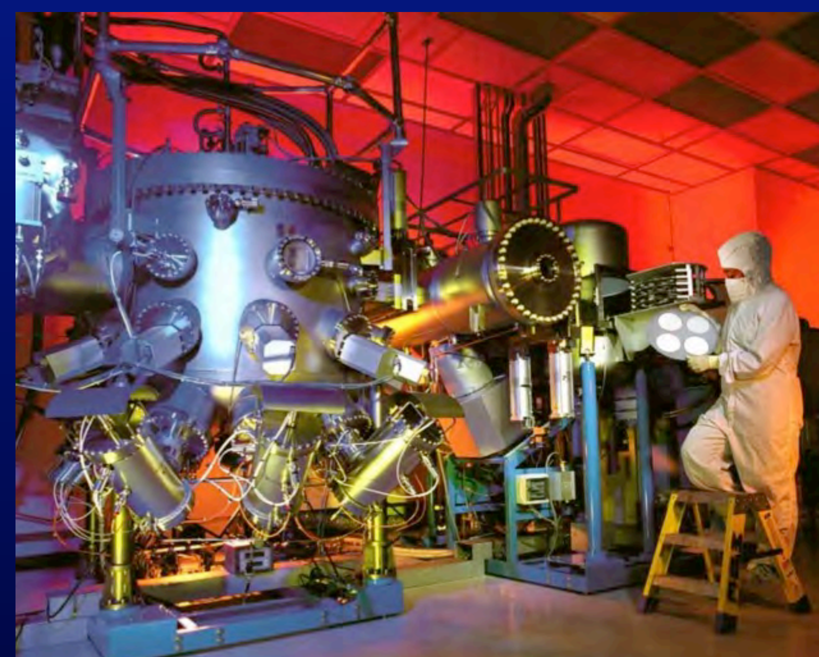

Production MBE Today
(courtesy of TRW)

MBE production tool performance data

HIGH YIELD

UNIFORMITIES / Wafer	Thickness < ± 0.5 %
	Composition < ± 0.5 %
	Doping < ± 1 %
REPRODUCIBILITY	Source material: supply consistency
	Stable process and monitoring: < 2%

HIGH THROUGHPUT

VERY HIGH UPTIME	> 94%, run 6 to 9 months, 7 days/wk, 24/24
RUN CAPABILITY	13x2'' or 5x3'', 4x6'' or 9x4'', (4x8'') 7x6''
RUN SWITCHING	less than 2 minutes (platen exchange)

Reflection High-Energy Electron Diffraction (RHEED) Oscillations

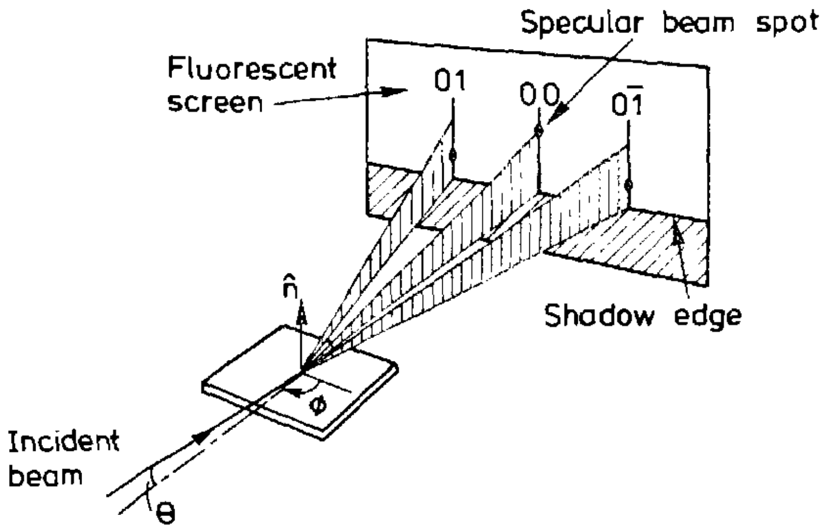

FIG. 1. Schematic diagram of RHEED geometry showing the incident beam at an angle θ to the surface plane; azimuthal angle φ. The elongated spots indicate the intersection of the Ewald sphere with the 01, 00, and 0$\bar{1}$ rods.

B. Bölger and P. K. Larsen, *Review of Scientific Instruments* **57** (1986) 1363-1367.

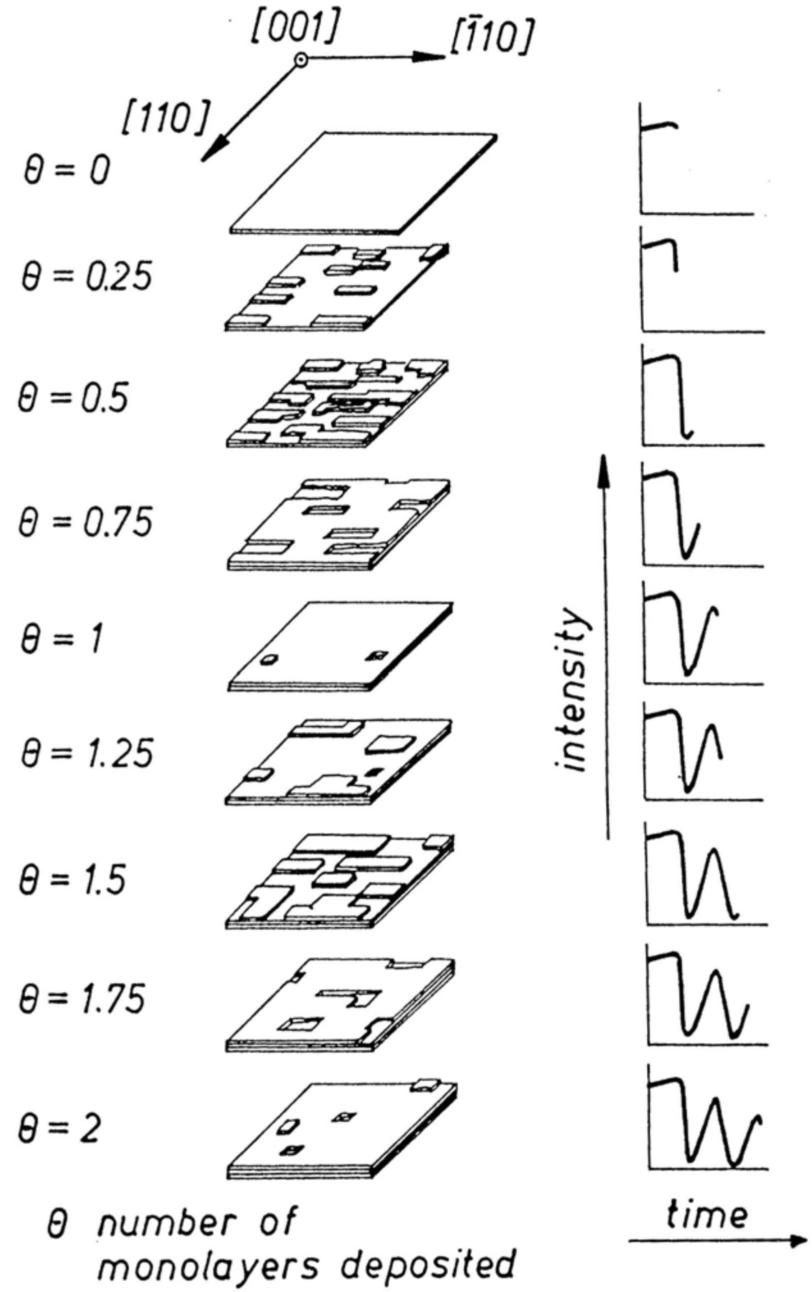

B.A. Joyce, P.J. Dobson, J.H. Neave, K. Woodbridge, J. Zhang, P.K. Larsen, and B Bölger, *Surface Science* **168** (1986) 423-438.

Quantum Cascade Laser

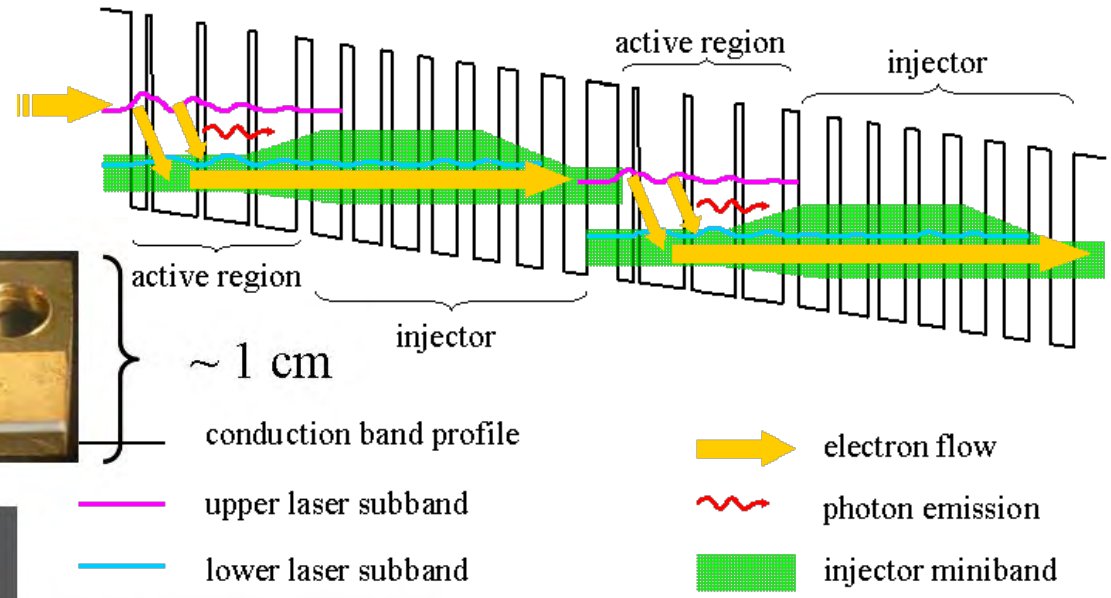

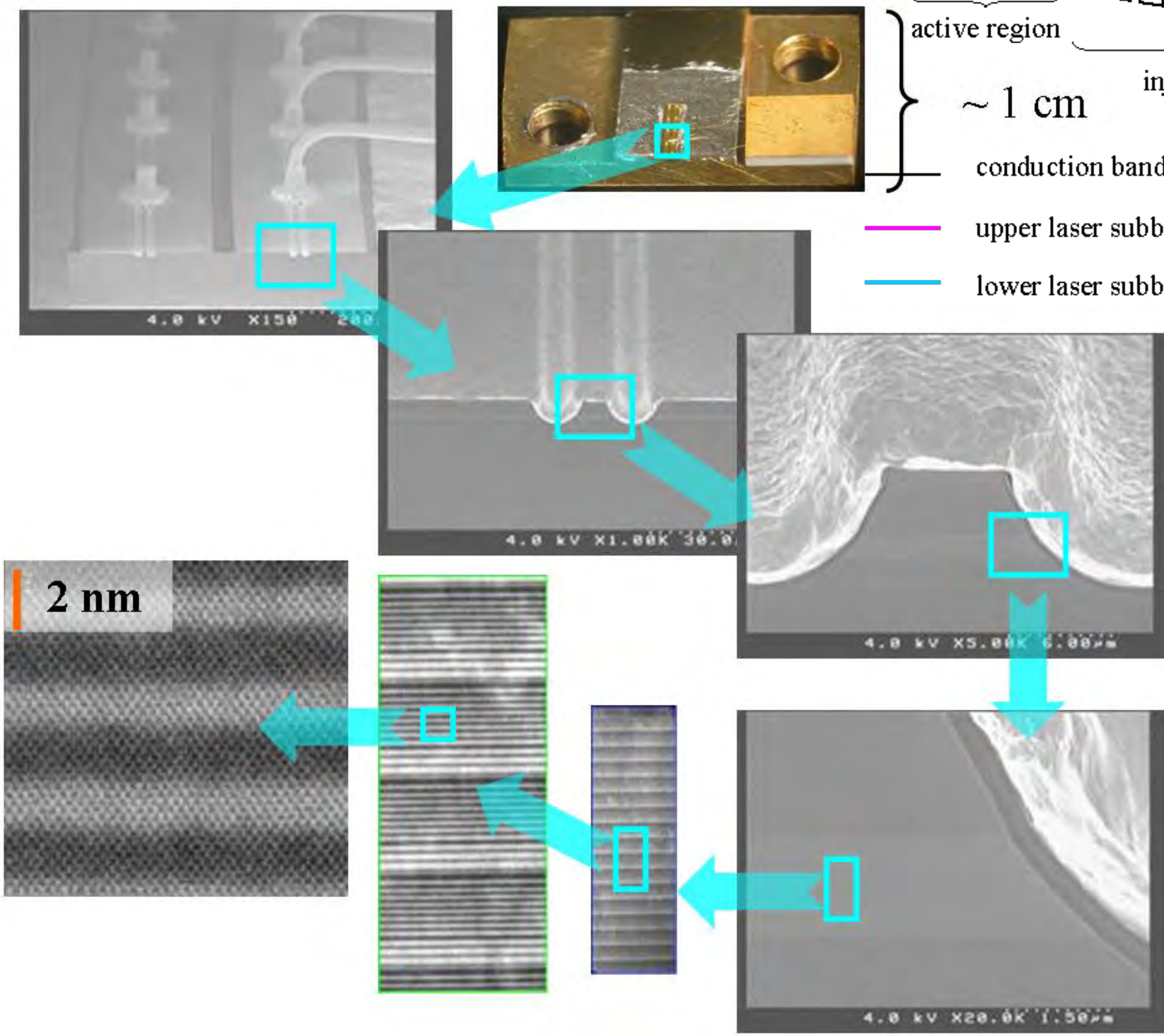

Yanbo Bai
http://www.yanbobai.com

What is MBE?

(a) Molecular-Beam Epitaxy

(b) Mega-Buck Evaporator

(c) Many Boring Evenings

(d) Mainly Broken Equipment

(e) All of the above

Outline

- What is MBE and what is it good for?
  Greatest hits of MBE

- How to grow your favorite oxide quantum material by MBE?
  Nuts and bolts of oxide MBE

- Oxide MBE growth of quantum materials
  Case studies—including Sr_2RuO_4

- How can I gain access to an oxide MBE if I don’t have one?
  Use PARADIM’s oxide MBE (+ ARPES + …)

MBE for Science / Technology

- 1998 Nobel Prize in Physics—Fractional Quantum Hall Effect
  - Horst Ludwig Störmer
  - Daniel Chee Tsui
  - Robert B. Laughlin

- 2000 Nobel Prize in Physics—Semiconductor Optoelectronics
  - Zhores Ivanovich Alferov
  - Herbert Kroemer

Modulation Doping

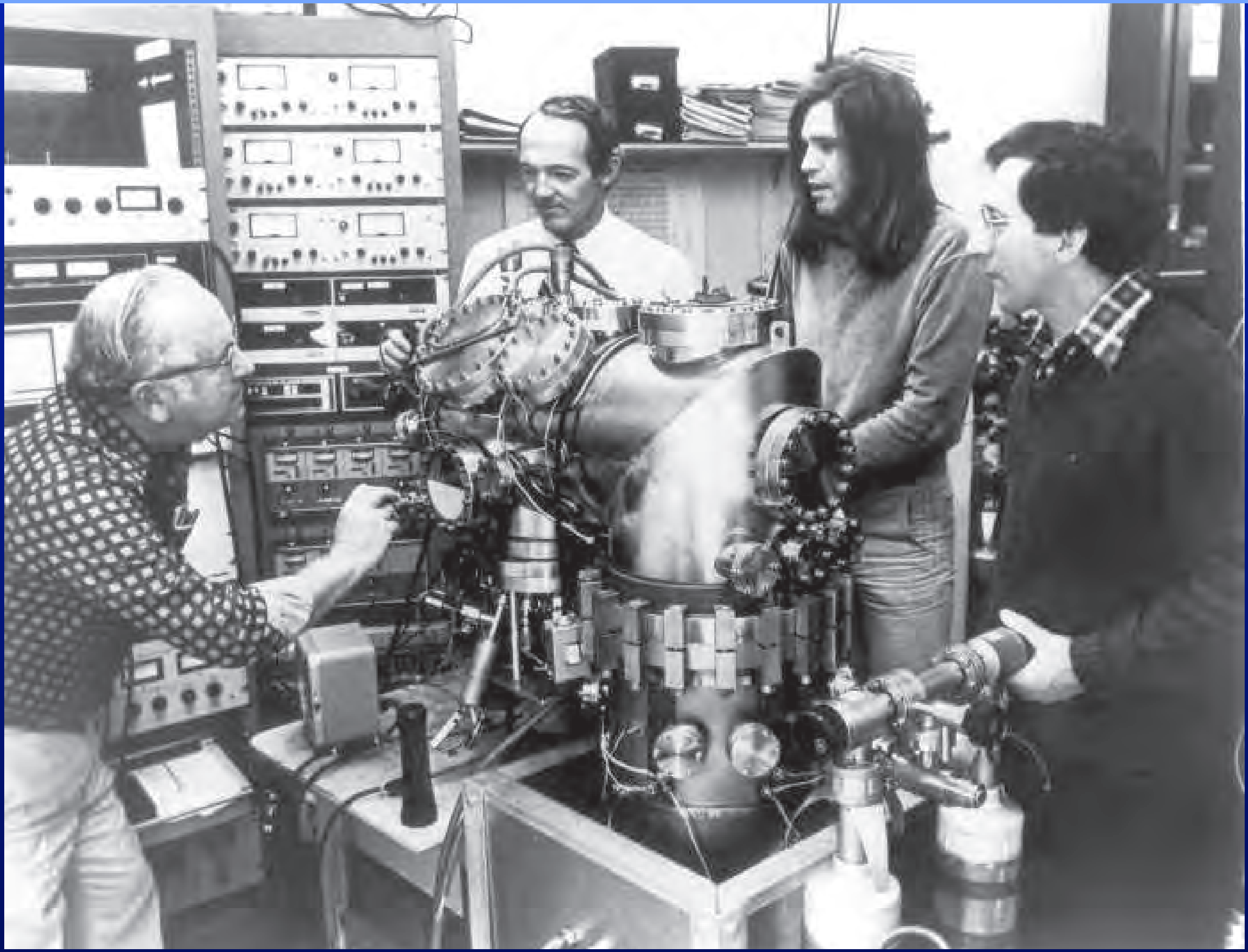

R. Dingle, H.L. Störmer, A.C. Gossard, and W. Wiegmann, *Applied Physics Letters* **33** (1978) 665-667.

Figure 2 Four pioneers of modulation doping gather around an early MBE machine at Bell Labs in 1978: (left–right) Willy Wiegmann, Art Gossard, Horst Störmer and Ray Dingle. Störmer and his Bell Labs colleague Daniel Tsui shared the Nobel prize for discovering the fractional quantum Hall effect in devices made by Gossard and co-workers with MBE.

W.P. McCray, *Nature Nanotechnology* **2** (2007) 259-261.

Modulation Doping

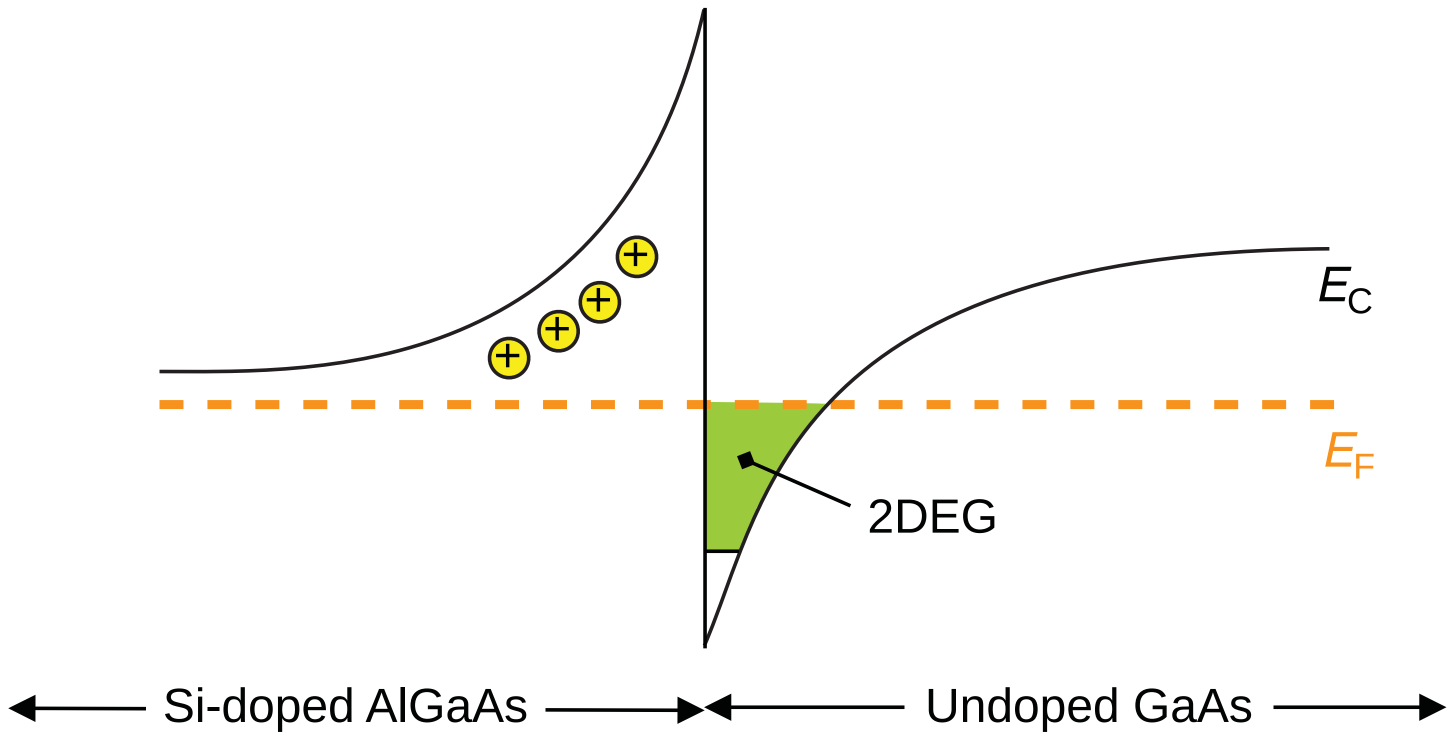

Figure 1. Band diagram showing the formation of a two-dimensional electron gas (2DEG) at a Si-doped AlGaAs–GaAs heterojunction. *Note:* E_F is the value of the Fermi energy, and E_C gives the energy of the conduction band edge.

J. Mannhart, D. H. A. Blank, H. Y. Hwang, A. J. Millis, and J.-M. Triscone, "Two-Dimensional Electron Gases at Oxide Interfaces," *MRS Bulletin* **33** (2008) 1027-1034.

Mobility Achieved with MBE

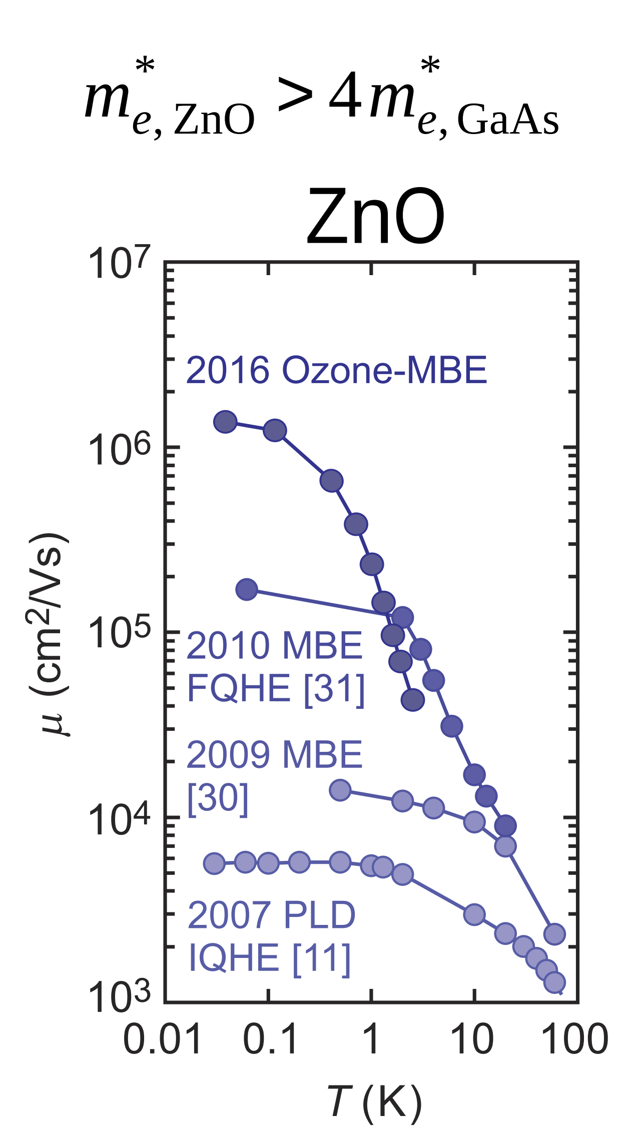

J. Falson, Y. Kozuka, M. Uchida, J. H. Smet, T.-H. Arima, A. Tsukazaki, and M. Kawasaki, *Scientific Reports* **6** (2016) 26598.

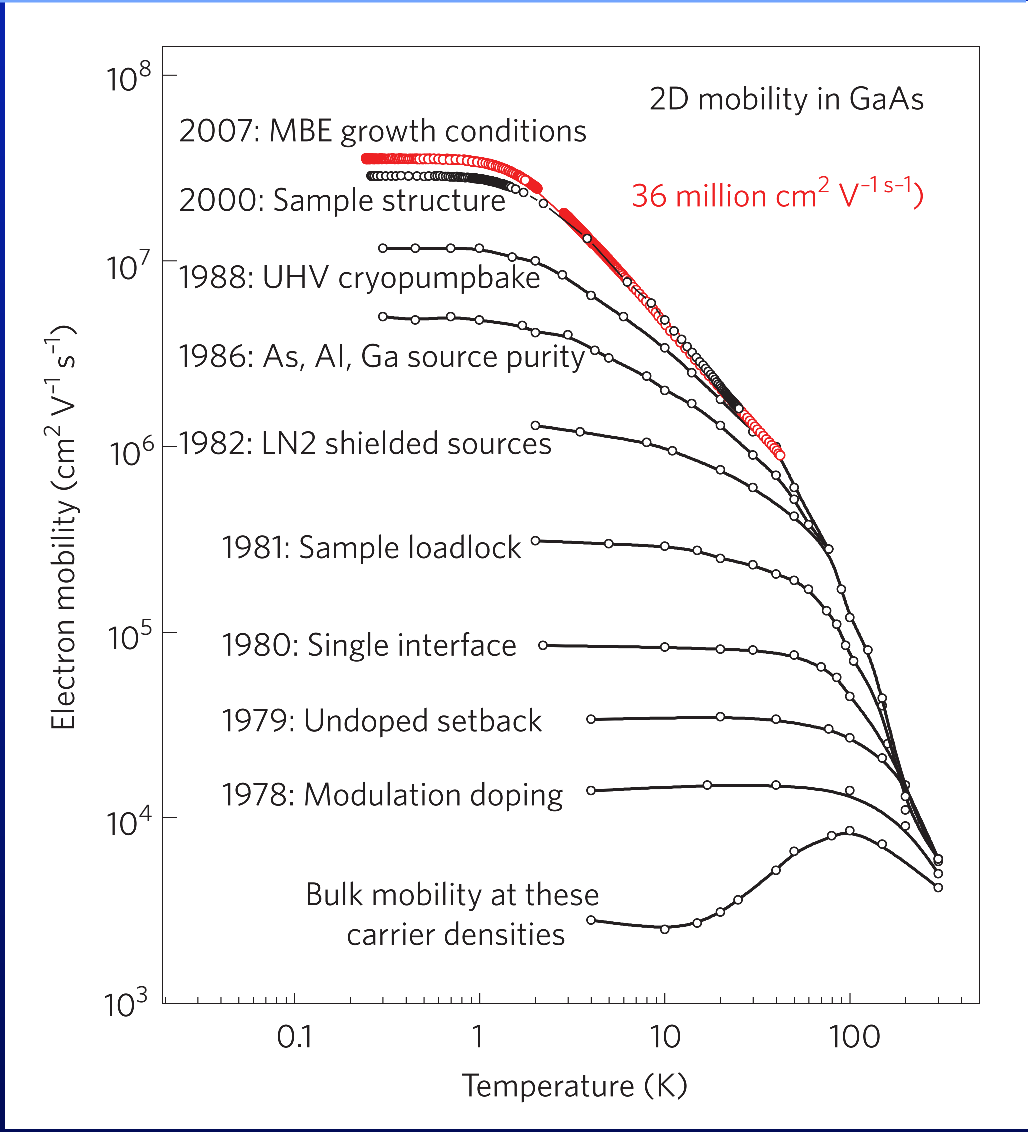

L. Pfeiffer and K.W. West, *Physics E* **20** (2003) 57-64.

D.G. Schlom and L.N. Pfeiffer, *Nature Materials* 9 (2010) 881-883.

Mobility Achieved with MBE

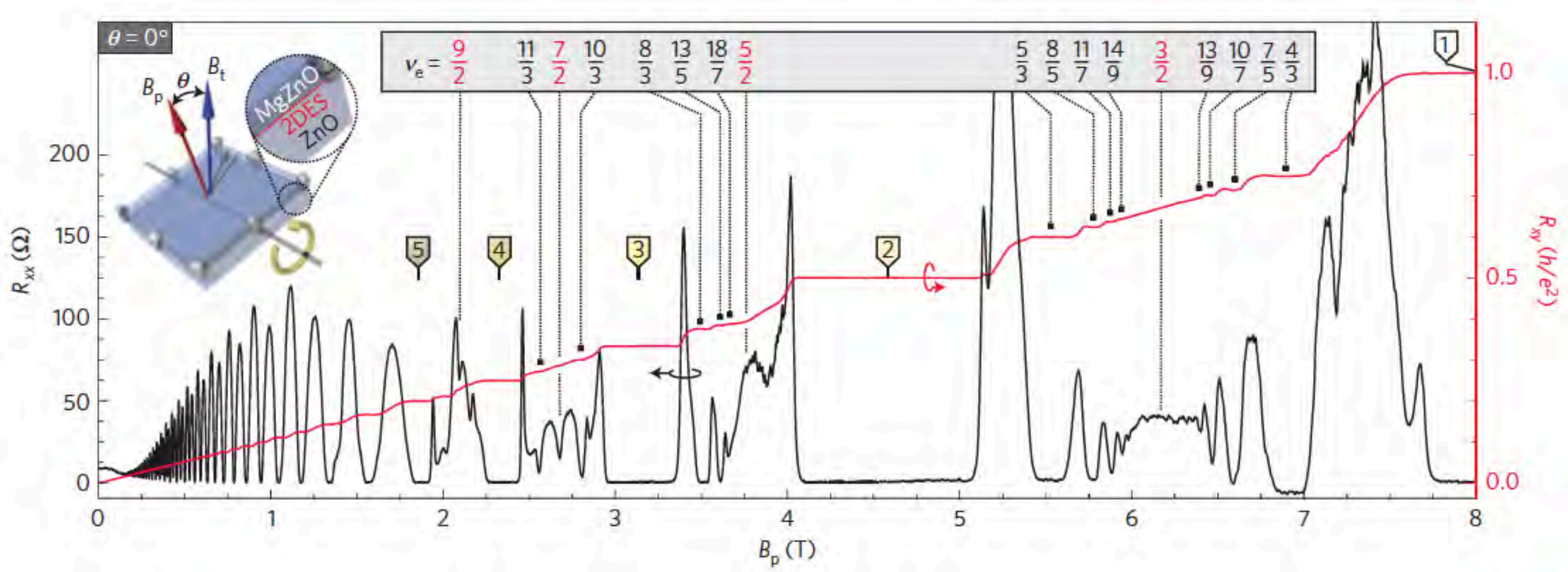

J. Falson, D. Maryenko, B. Friess, D. Zhang, Y. Kozuka, A. Tsukazaki, J. H. Smet, and M. Kawasaki, *Nature Physics* **11** (2015) 347–351.

MBE of Quantum Materials

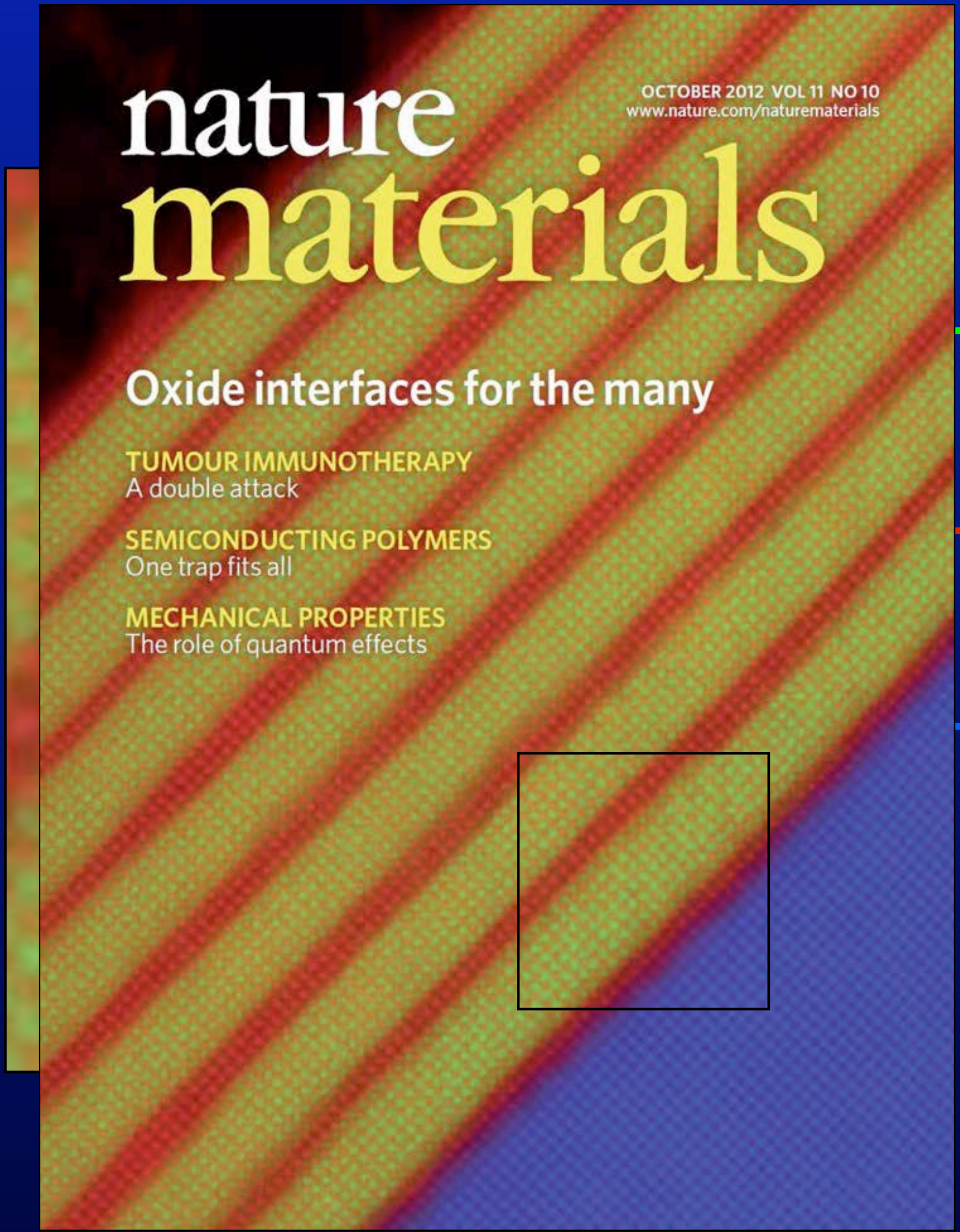

$(SrRuO_3)_1$ / $(SrTiO_3)_5$
Superlattice

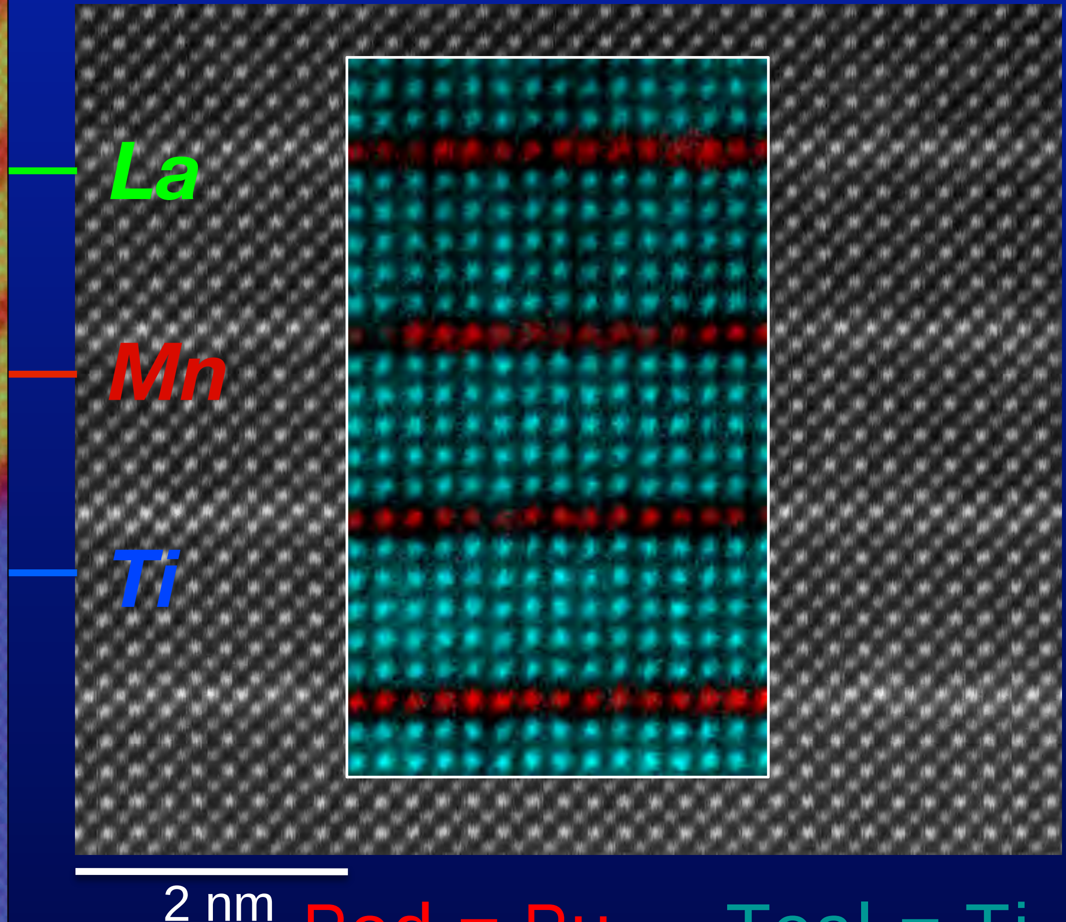

Red = Ru Teal = Ti

E.J. Monkman, C. Adamo, J.A. Mundy, D.E. Shai, J.W. Harter, D. Shen, B. Burganov, D.A. Muller, D.G. Schlom, and K.M. Shen, *Nature Materials* **11** (2012) 855-859.

Transport of $SrRuO_3$ Films

Best PLD Film

$\rho_{300\ K}$ / $\rho_{10\ K}$ = 14.1

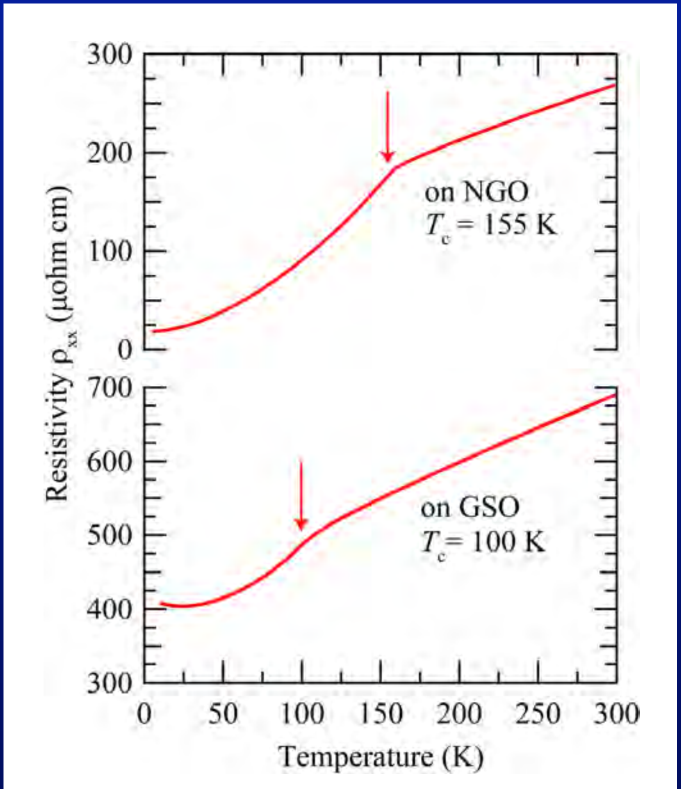

~20 nm $SrRuO_3$ / (110) $NdGaO_3$

D. Kan, R. Aso, H. Kurata, and Y. Shimakawa,
J. Appl. Phys. **113** (2013) 173912 .

Best MBE Film

$\rho_{300\ K}$ / $\rho_{4\ K}$ = 76

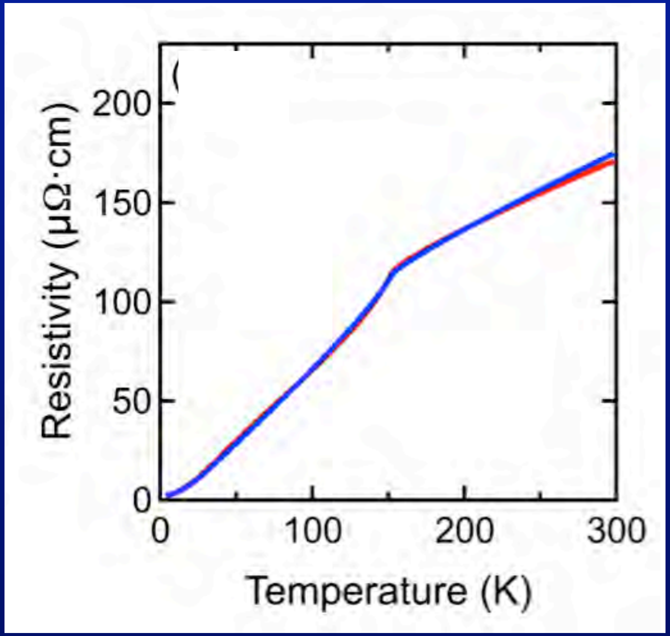

32 nm $SrRuO_3$ / (100) $SrTiO_3$

H.P. Nair, Y. Liu, J.P. Ruf, N.J. Schreiber,S-L. Shang,
D.J. Baek, B.H. Goodge, L.F. Kourkoutis,
Z.K. Liu, K.M. Shen, and D.G. Schlom,
APL Materials **6** (2018) 046101.

Outline

- What is MBE and what is it good for?
  Greatest hits of MBE

- How to grow your favorite oxide quantum material by MBE?
  Nuts and bolts of oxide MBE

- Oxide MBE growth of quantum materials
  Case studies—including Sr_2RuO_4

- How can I gain access to an oxide MBE if I don't have one?
  Use PARADIM's oxide MBE (+ ARPES + …)

Nuts and Bolts of Oxide MBE

- Mean Free Path (maximum P_{O_2})
- Minimum P_{O_2}, need for P_{O_3}, Optimal T_{sub}
- MBE System, Sources, and Crucibles
- Composition Control
    - Adsorption-Controlled Growth
    - Flux-Controlled Growth
- Substrates

Maximum O_2 Pressure for MBE

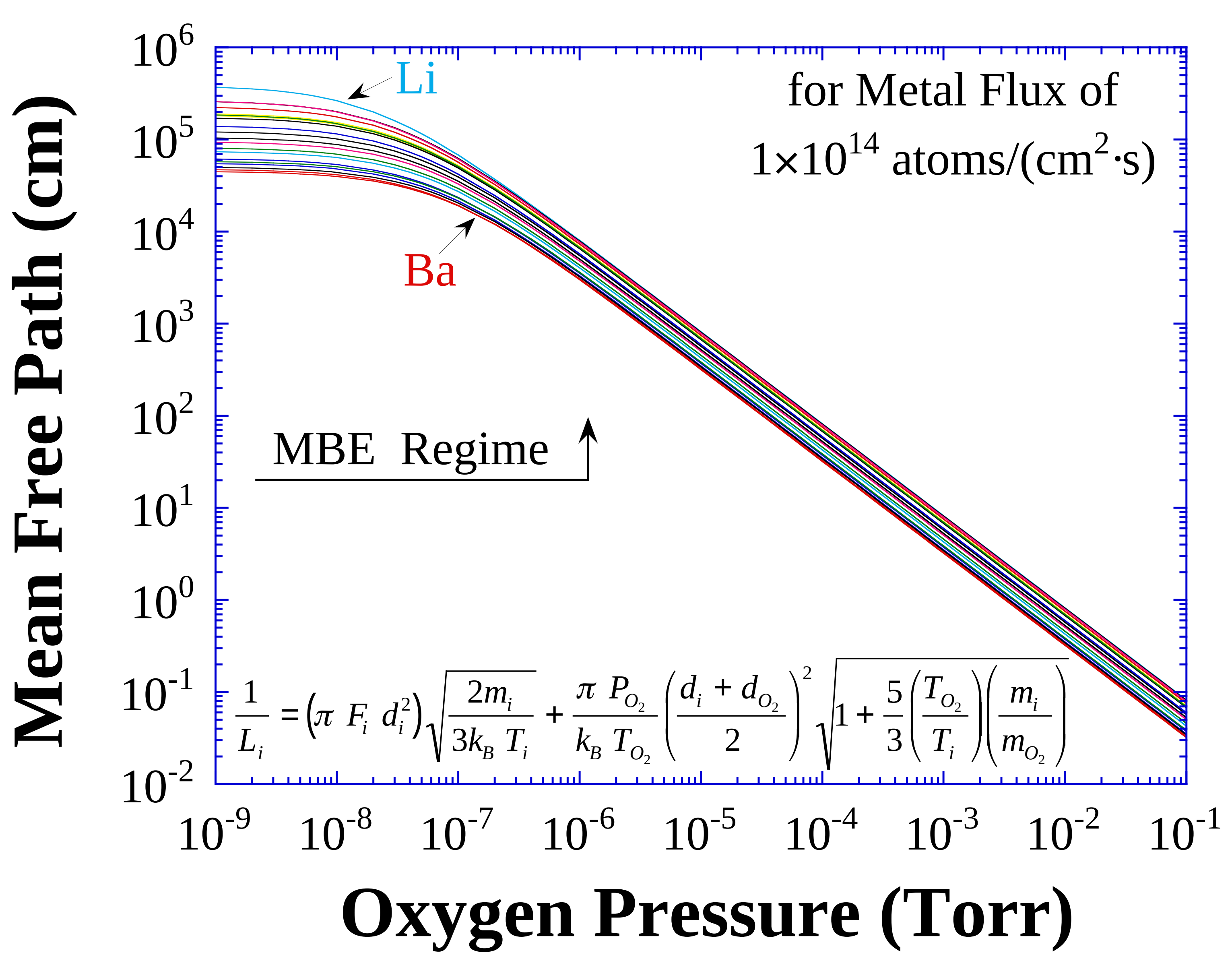

D.G. Schlom and J.S. Harris, Jr., "MBE Growth of High T_c Superconductors," in: Molecular Beam Epitaxy: Applications to Key Materials, edited by R.F.C. Farrow (Noyes, Park Ridge, 1995), pp. 505-622.

O_2 Needed to Oxidize Constituents

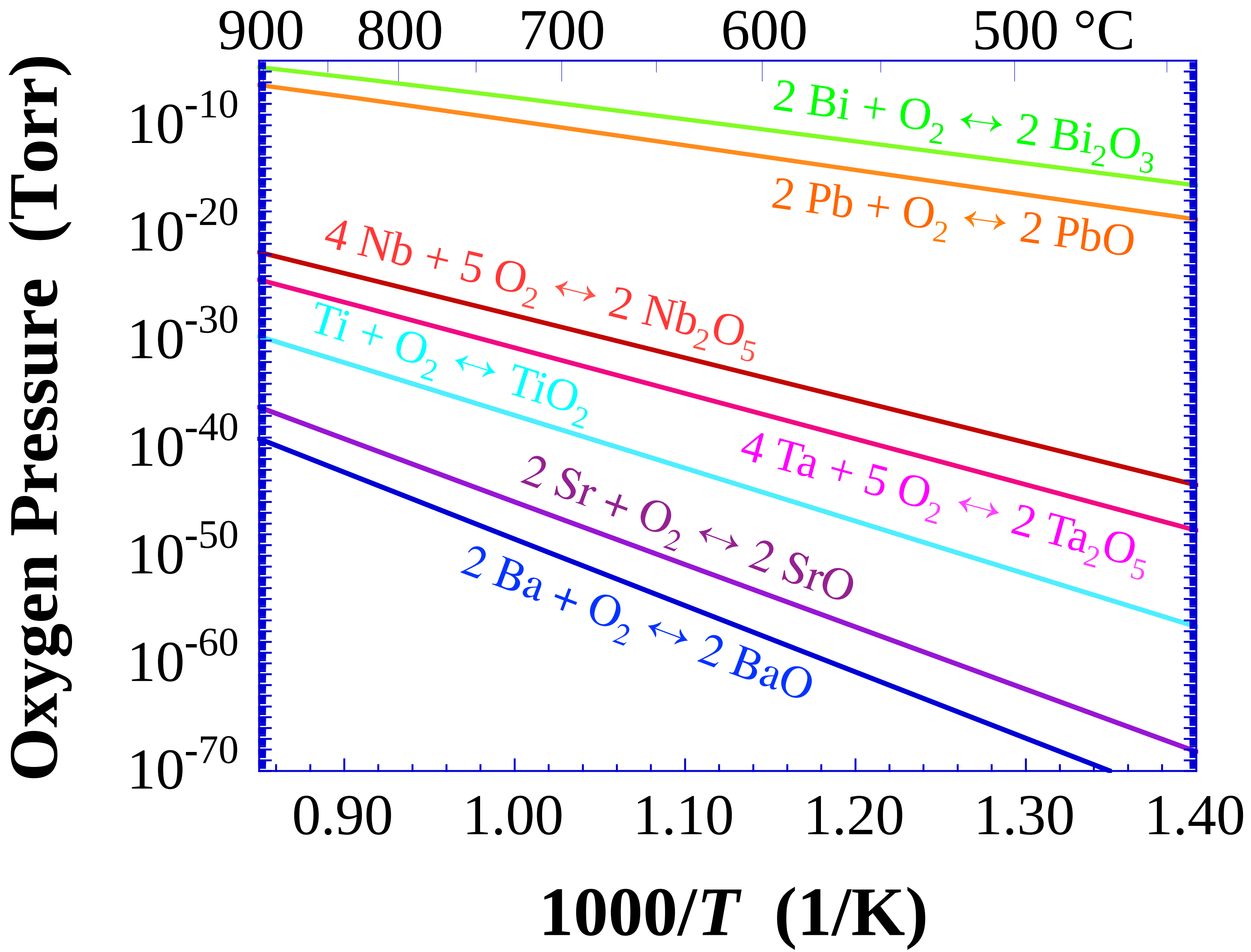

O_2 Needed to Oxidize Cuprates

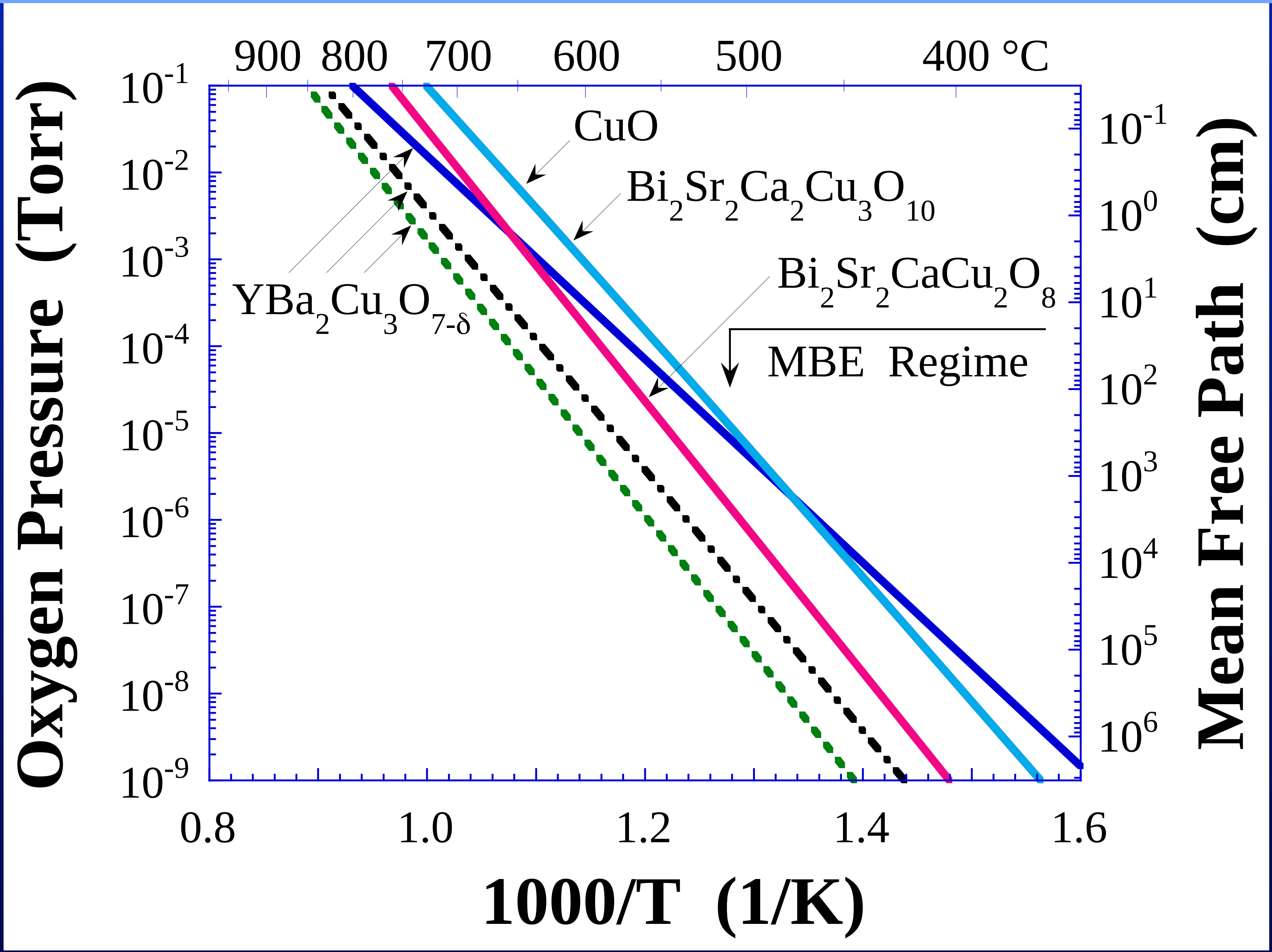

D.G. Schlom and J.S. Harris, Jr., "MBE Growth of High T_c Superconductors," in: Molecular Beam Epitaxy: Applications to Key Materials, edited by R.F.C. Farrow (Noyes, Park Ridge, 1995), pp. 505-622.

Superior Oxidants

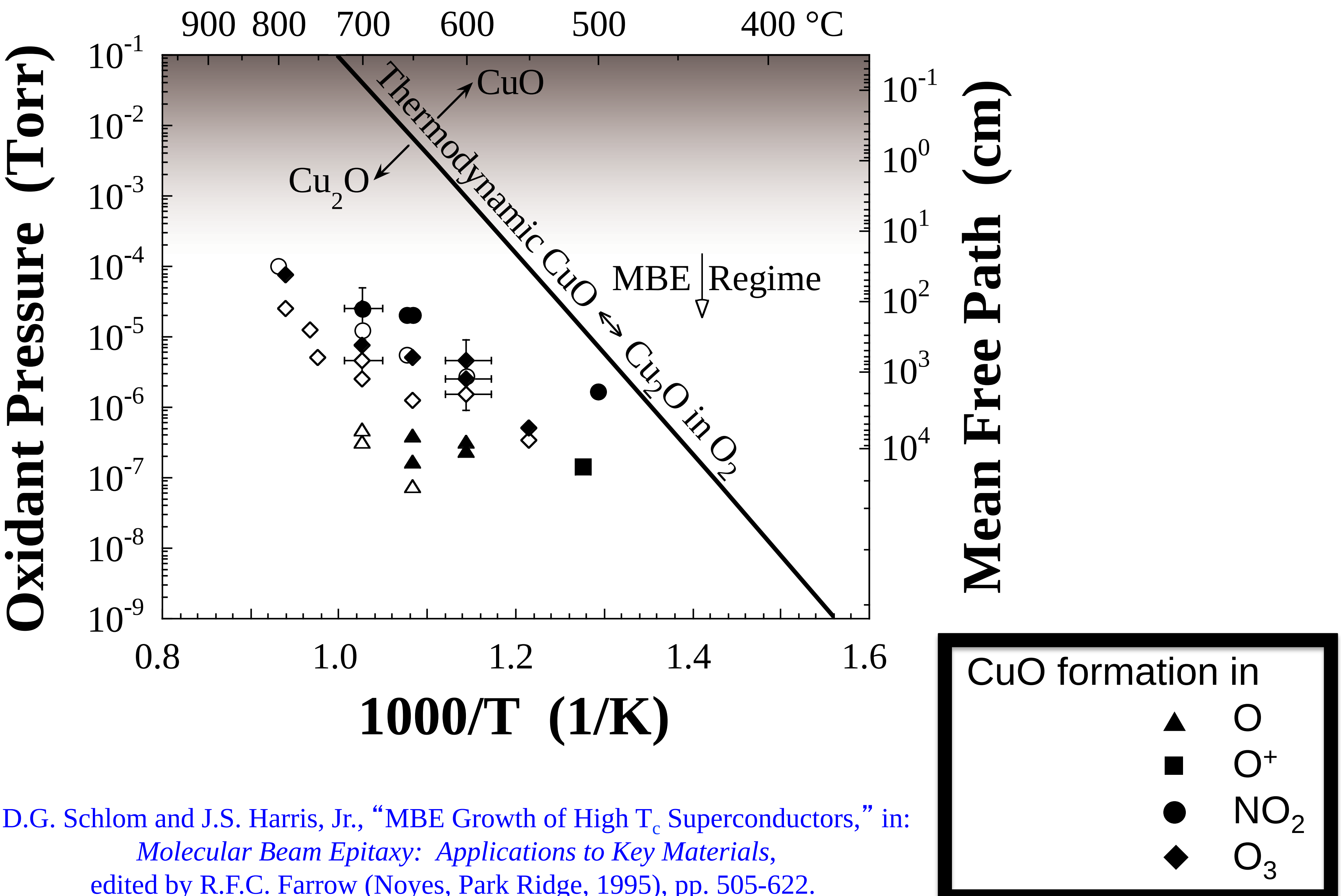

D.G. Schlom and J.S. Harris, Jr., "MBE Growth of High T_c Superconductors," in: *Molecular Beam Epitaxy: Applications to Key Materials,* edited by R.F.C. Farrow (Noyes, Park Ridge, 1995), pp. 505-622.

Oxygen vs. Ozone

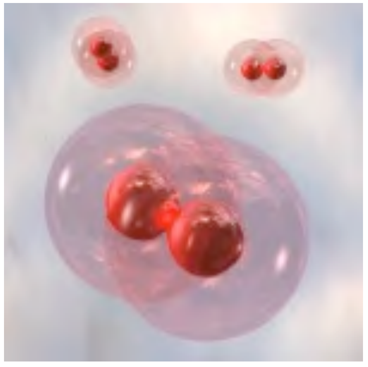

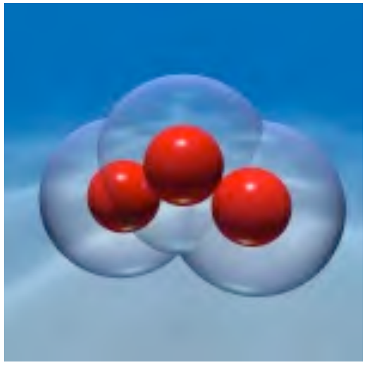

Oxygen:

- Easy to use – directly from the cylinder
- Depending on material, films are oxygen-deficient

Ozone from ozone generator:

- Around 15 wt% O_3 in O_2
- As O_3 easily decomposes, one O_3 is similar to one O radical
- Higher wt% not achievable, saturation of O_3 concentration

Distilled ozone:

- Can provide 80-100 wt% pure O_3
- Better film oxidation, wider process window
- But: Gas is explosive above 10 Torr (absolute), liquid is explosive and shock-sensitive

Vapor Pressure Oxygen vs. Ozone

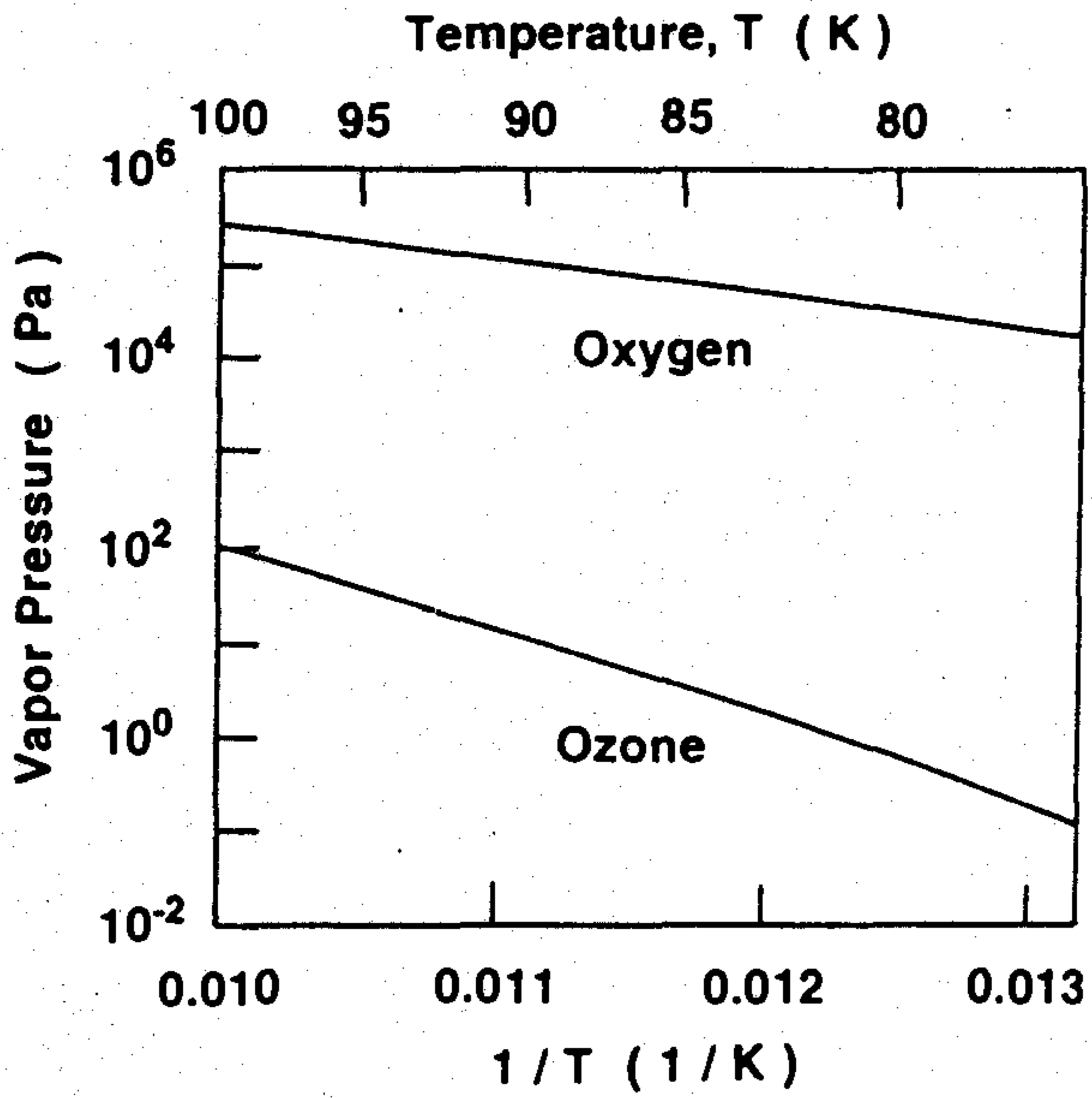

FIG. 4. Vapor pressure of ozone and oxygen as a function of temperature.

S. Hosokawa, and S. Ichimura, "Ozone Jet Generator as an Oxidizing Reagent Source for Preparation of Superconducting Oxide Thin Film," *Review of Scientific Instruments* **62** (1991) 1614-1619.

Ozone Safety Concerns

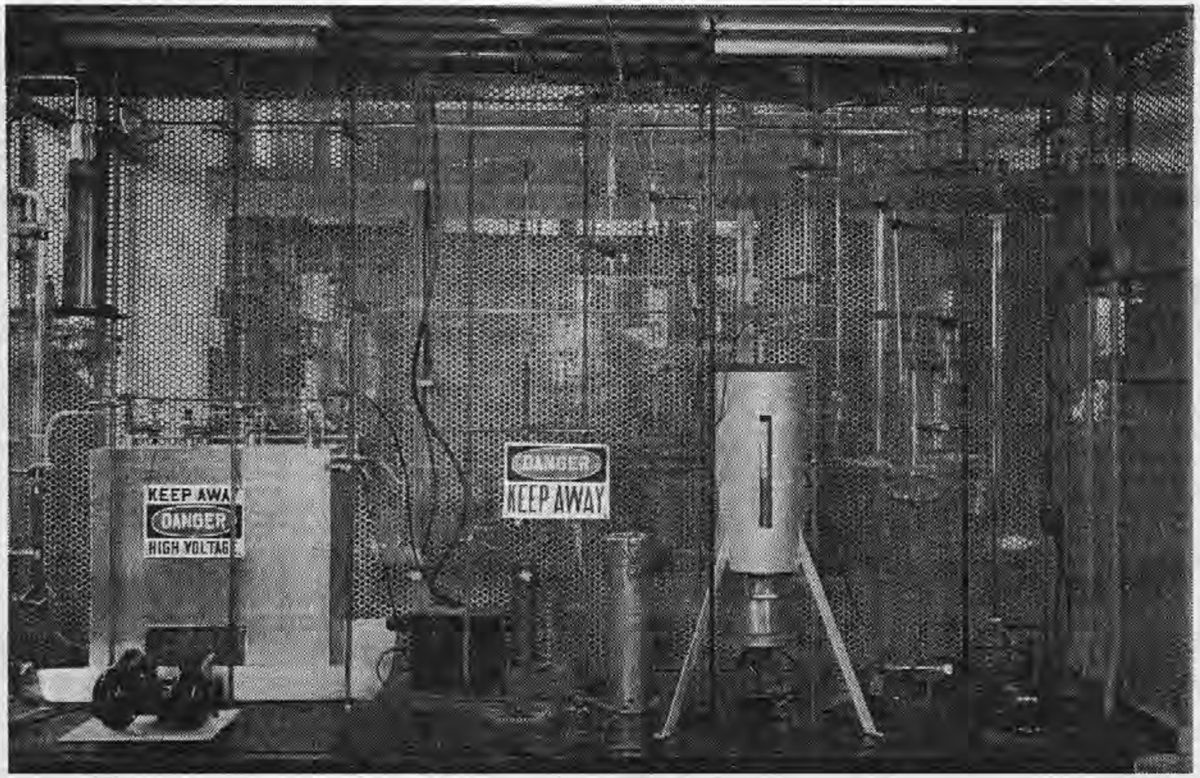

Figure 4. Ozone system

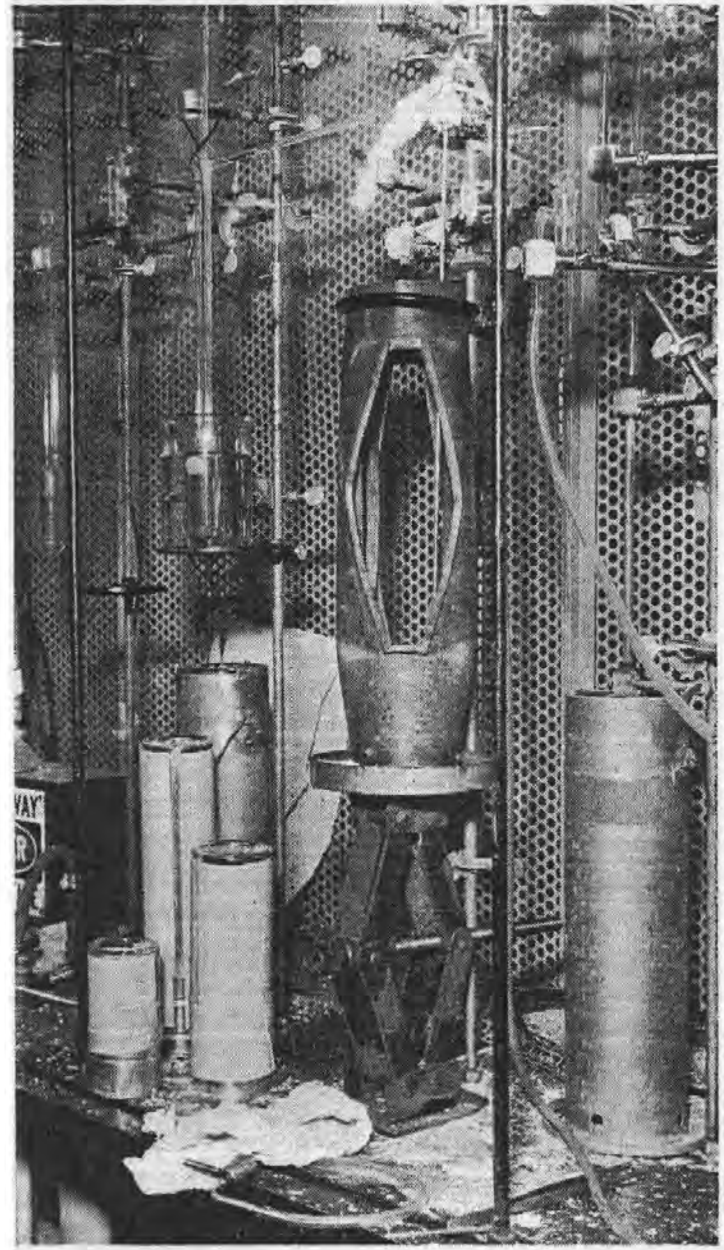

Figure 5. Apparatus after explosion

A.C. Jenkins, "Laboratory Techniques for Handling High-Concentration Liquid Ozone," in: *Ozone Chemistry and Technology*, Vol. 21 of Advances in Chemistry Series, (American Chemical Society, Washington, D.C., 1959) pp. 13-21.

Ozone Safety Concerns

OZONE FOR ROCKETS

Concentrated liquid ozone has been proposed as a rocket fuel by Prof. Clark E. Thorp of the Illinois Institute of Technology, who recently disclosed advances made at the Institute by which ozone can be handled with safety. Ozone is a form of oxygen with three atoms to the molecule instead of two as in ordinary life-supporting oxygen. By demonstrating that it can be safely manufactured, Professor Thorp stated, the door has been opened for tonnage production. During World War II, German scientists worked overtime on an ozone-propelled rocket designed to bombard New York City from European launching platforms. But they were unable to discover the secret of handling ozone without spontaneous detonation.

"Ozone for Rockets," *Ordnance: The Journal of the Army Ordnance Association* **36** [187] (July-August 1951) pp. 108-110.

Ozone Distillation (U. Minnesota)

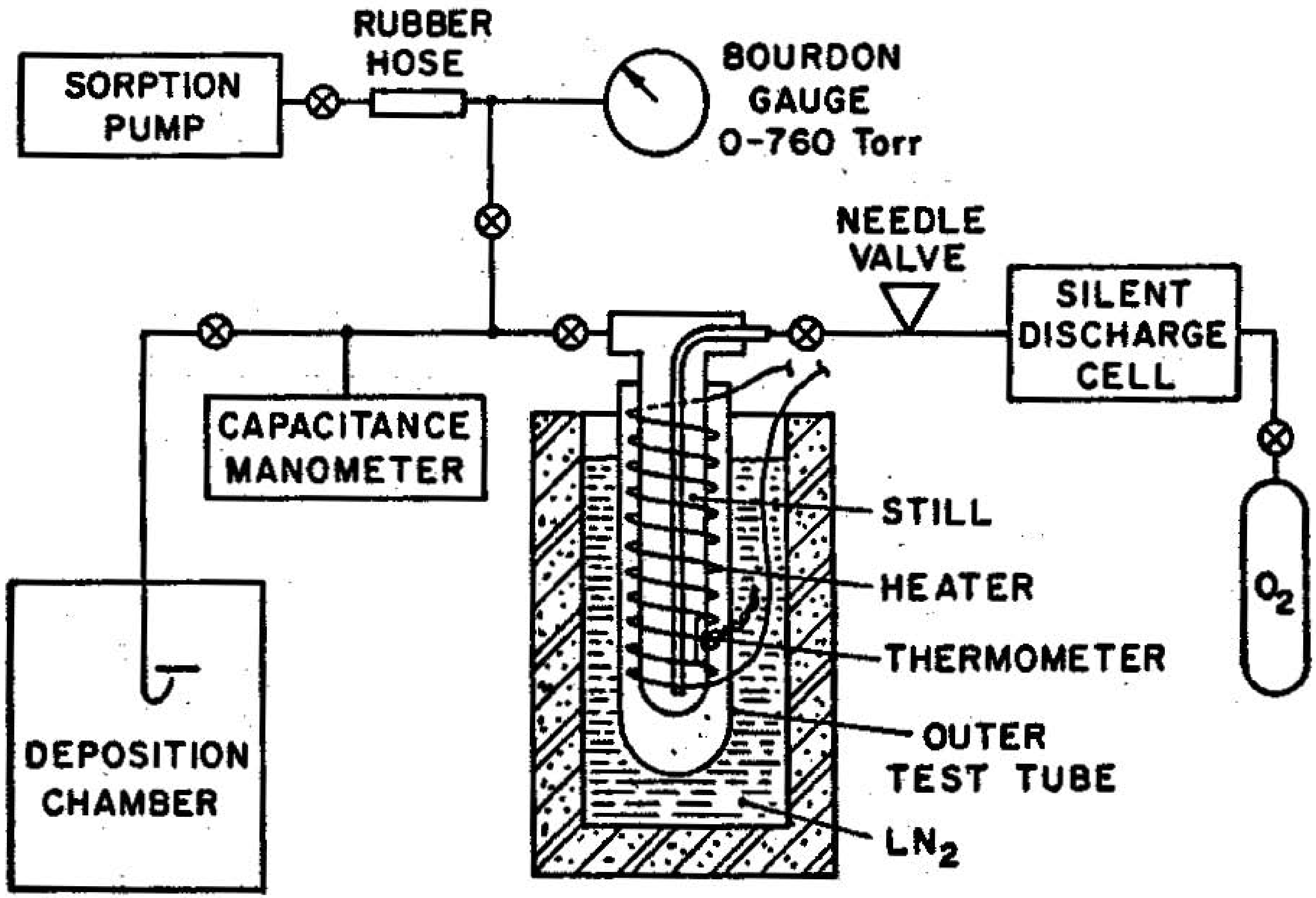

Fig. 1. Ozone-production and storage apparatus. During production of ozone, the still heater is off and the outer test tube surrounding the still is filled with liquid nitrogen.

D.D. Berkley, A.M. Goldman, B.R. Johnson, J. Morton, and T. Wang, "Techniques for the Growth of Superconducting Oxide Thin Films Using Pure Ozone Vapor," *Review of Scientific Instruments* **60** (1989) 3769-3774.

Ozone in Silica Gel—Union Carbide

Separation of Ozone from Oxygen by a Sorption Process

G. A. COOK, A. D. KIFFER, C. V. KLUMPP, A. H. MALIK, and L. A. SPENCE

Research and Development Laboratory, Linde Co., A Division of Union Carbide Corp., Tonawanda, N. Y.

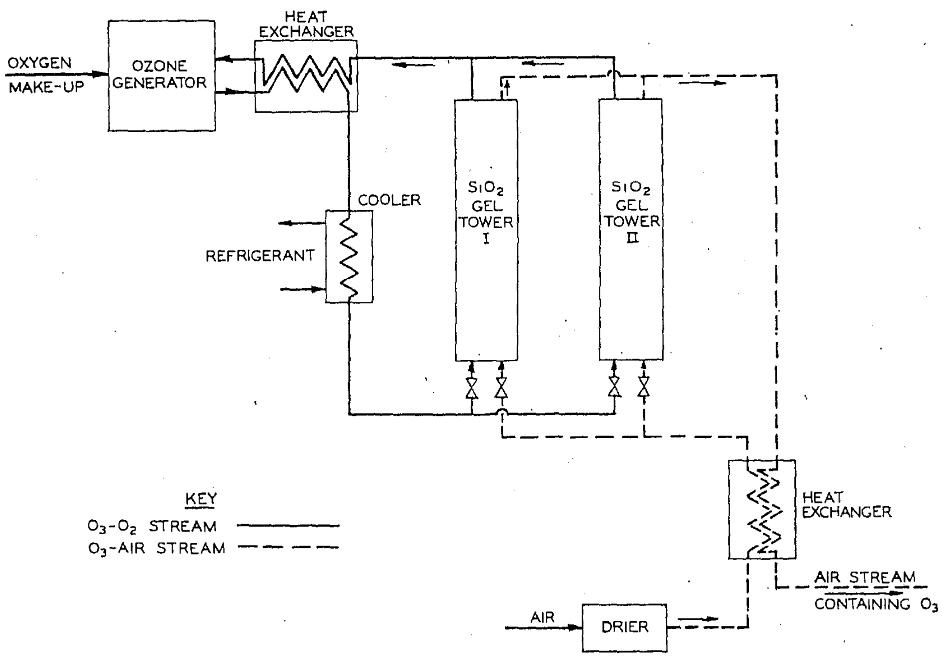

Figure 7. Simplified flow diagram for two-stage transfer process

Ozone is separated from oxygen by adsorption on refrigerated silica gel, followed by desorption, either in pure form at reduced pressure, or diluted by air, nitrogen, argon, or other gas not strongly adsorbed on silica gel. This is a practical method, free from hazard when correctly performed.

G.A. Cook, A.D. Kiffer, , C.V. Klumpp, A.H. Malik, and L.A. Spence, "Separation of Ozone from Oxygen by a Sorption Process," in: *Ozone Chemistry and Technology*, Vol. 21 of Advances in Chemistry Series, (American Chemical Society, Washington, D.C., 1959) pp. 44-52.

Ozone in Silica Gel—Union Carbide

Safety Tests

An electric spark was passed between two tungsten electrodes within the gel bed. No explosions took place at −105° C. with loadings as high as 21 grams of ozone per 100 grams of gel.

A piece of fine iron wire was placed in the bed of gel and ignited by passing an electric current through it. With a loading of 9 grams of ozone per 100 grams of gel, a test was made at −78° C. After ignition of the wire, a glow in the vessel was observed, but no explosion took place. With a loading of 20 grams of ozone per 100 grams of gel at −105° C., a dull pop was heard when the wire was ignited, most of the ozone changed to oxygen, and the gel was extensively pulverized. The glass container was broken but not shattered.

G.A. Cook, A.D. Kiffer, , C.V. Klumpp, A.H. Malik, and L.A. Spence,
"Separation of Ozone from Oxygen by a Sorption Process," in: *Ozone Chemistry and Technology*,
Vol. 21 of Advances in Chemistry Series, (American Chemical Society, Washington, D.C., 1959) pp. 44-52.

Ozone in Silica Gel

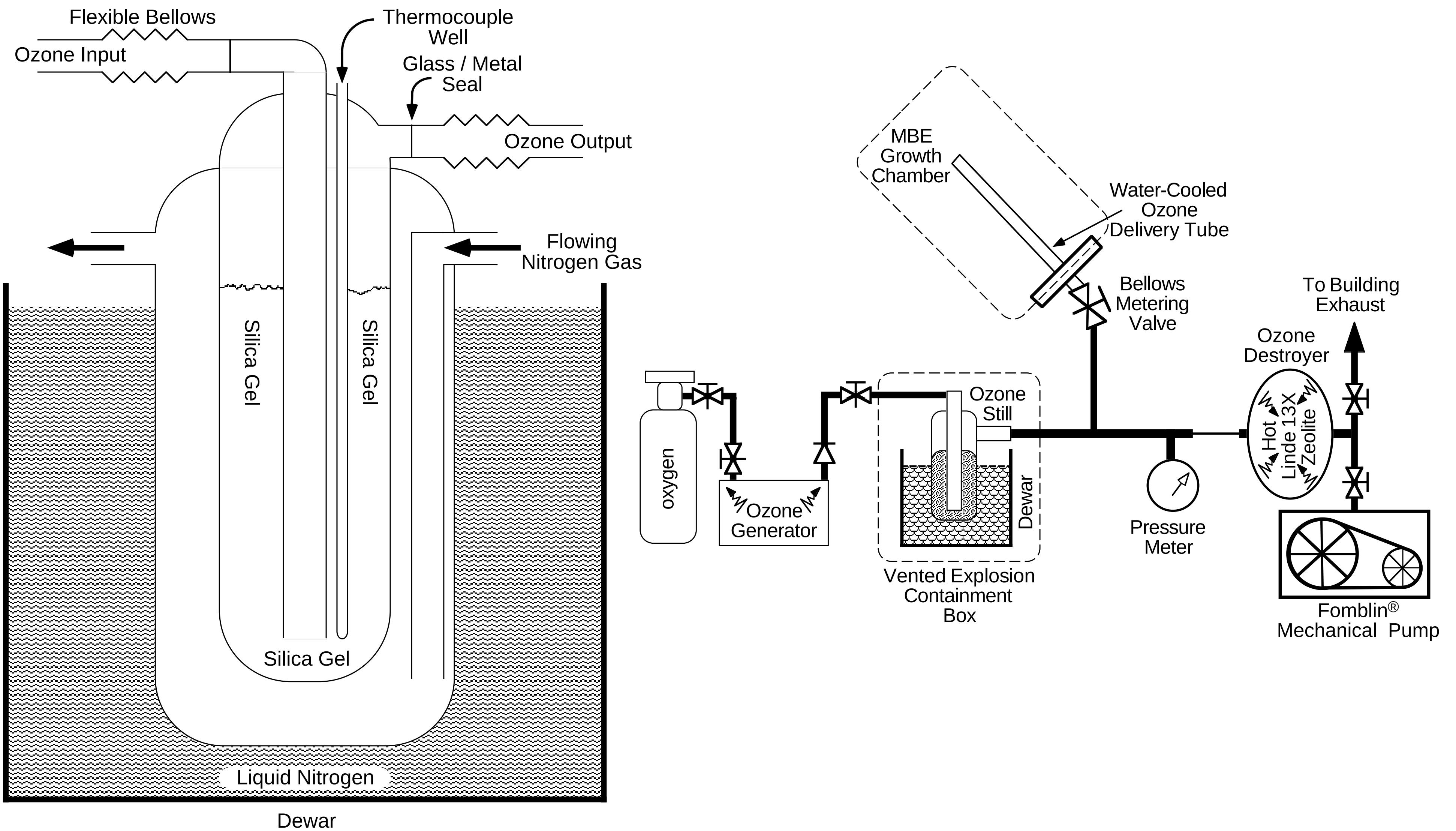

D.G. Schlom and J.S. Harris, Jr., "MBE Growth of High T_c Superconductors," in: *Molecular Beam Epitaxy: Applications to Key Materials*, edited by R.F.C. Farrow (Noyes, Park Ridge, 1995), pp. 505-622.

Process Control

- Safety committee requirements led to development of fully integrated process controller
- Controller monitors all process equipment and parameters
- Countermeasures if close to critical limit
- Self-test of equipment before process start
- Fully automated operation
- No need to manually watch ozone process, user can focus on MBE growth!!!

Ozone System Passivation

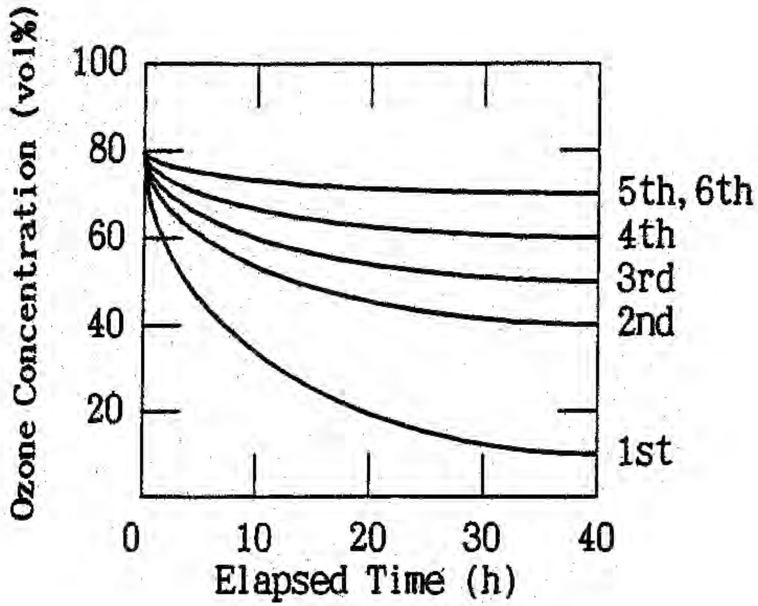

Fig. 2. Ozone concentration decay during ozone passivation.

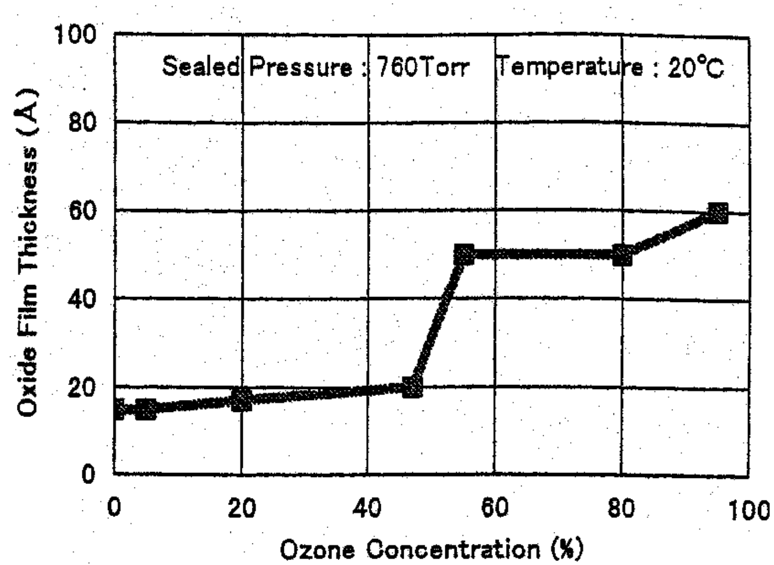

Fig. 4. Relationship of ozone concentration with thickness of passivated film formed at atmospheric pressure and 20°C.

K. Koike, G. Inoue, T. Takata, and T. Fukuda,
Ozone Passivation Technique for Corrosive Gas Distribution System,"
Japanese Journal of Applied Physics **36** (1997) 7437-7441.

Pros and Cons of Ozone

- Pros
  - Excellent Oxidant
    (about 1000× more powerful than O_2)
  - 80% Ozone (+20% O_2) Delivery Possible to the Substrate
  - No Energetic Species (thermal ozone beam)
  - Inexpensive (if you make it yourself)

- Cons
  - Safety (Ozone still issues)
  - Safety (Pump issues)
  - Need Ozone-Compatible UHV Leak Valve
  - Need to Passivate Ozone System

Nuts and Bolts of Oxide MBE

- Mean Free Path (maximum P_{O_2})
- Minimum P_{O_2}, need for P_{O_3}, Optimal T_{sub}
- MBE System, Sources, and Crucibles
- Composition Control
    - Adsorption-Controlled Growth
    - Flux-Controlled Growth
- Substrates

Surface vs. Bulk Diffusion

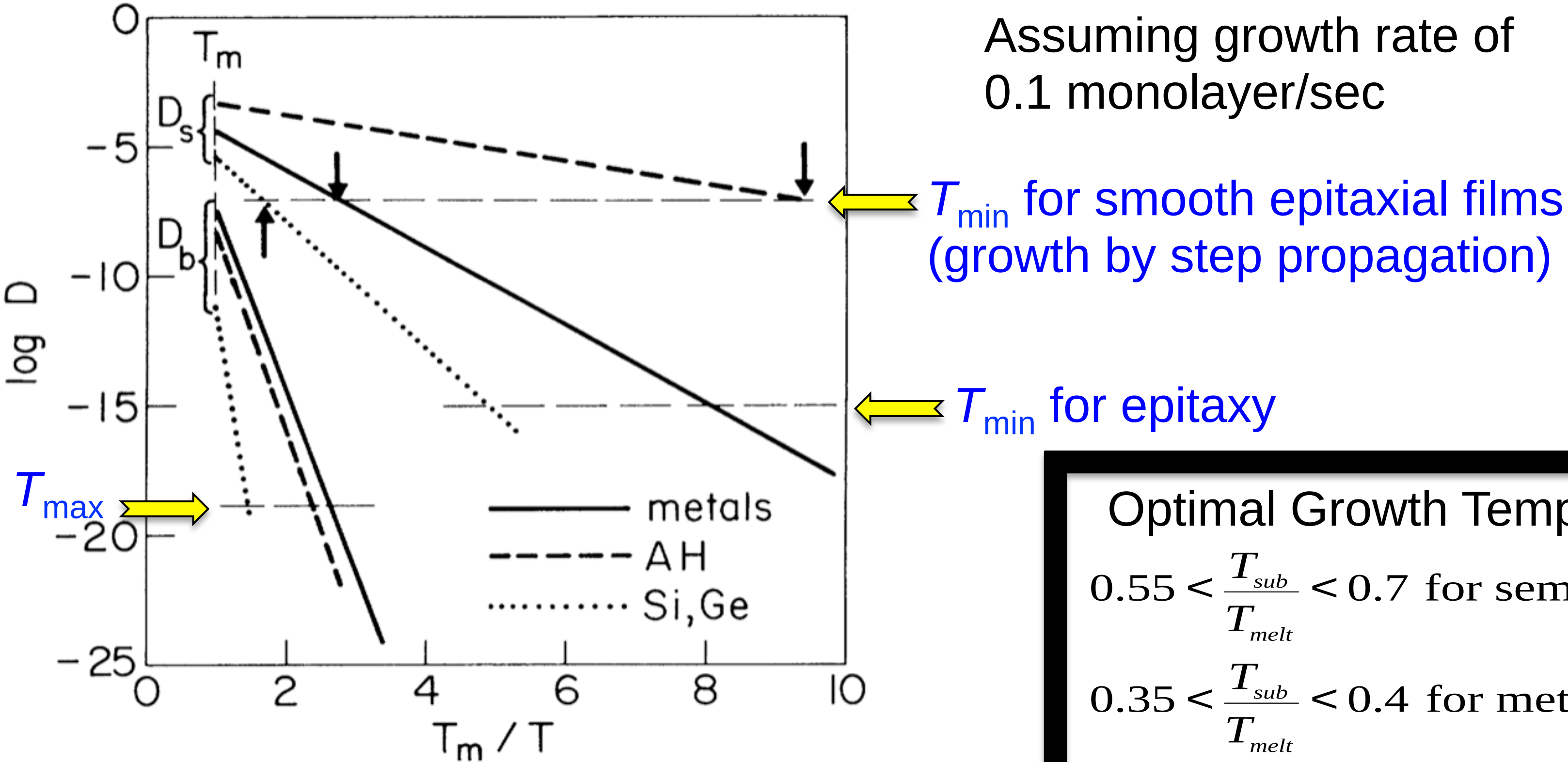

FIG. 6. Diagram showing deduced global dependences of surface and bulk diffusion coefficients, D_s and D_b, on T_m/T for metals (solid lines), elemental semiconductors (dotted lines), and salts (dashed lines). The construction is described in the text. Smooth flat interfaces generally require $D_s \gtrsim 10^{-8}$–10^{-7} cm^2/sec, which fixes the lowest growth temperatures (arrows) as $\sim 3T_m/8$, $0.55T_m$, and $0.1T_m$ in the three cases. RHEED oscillations are expected for $D_s \gtrsim 10^{-15}$ cm^2/sec and bulk interdiffusion for $D_b \gtrsim 10^{-19}$ cm^2/sec.

Assuming growth rate of 0.1 monolayer/sec

Optimal Growth Temperatures

$$0.55 < \frac{T_{sub}}{T_{melt}} < 0.7 \text{ for semiconductors}$$

$$0.35 < \frac{T_{sub}}{T_{melt}} < 0.4 \text{ for metals}$$

$$0.1 < \frac{T_{sub}}{T_{melt}} < 0.4 \text{ for simple ceramics}$$

M.H. Yang and C.P. Flynn, *Physical Review Letters* **62** (1989) 2476-2479.

Universal Diffusion Behavior of Metals

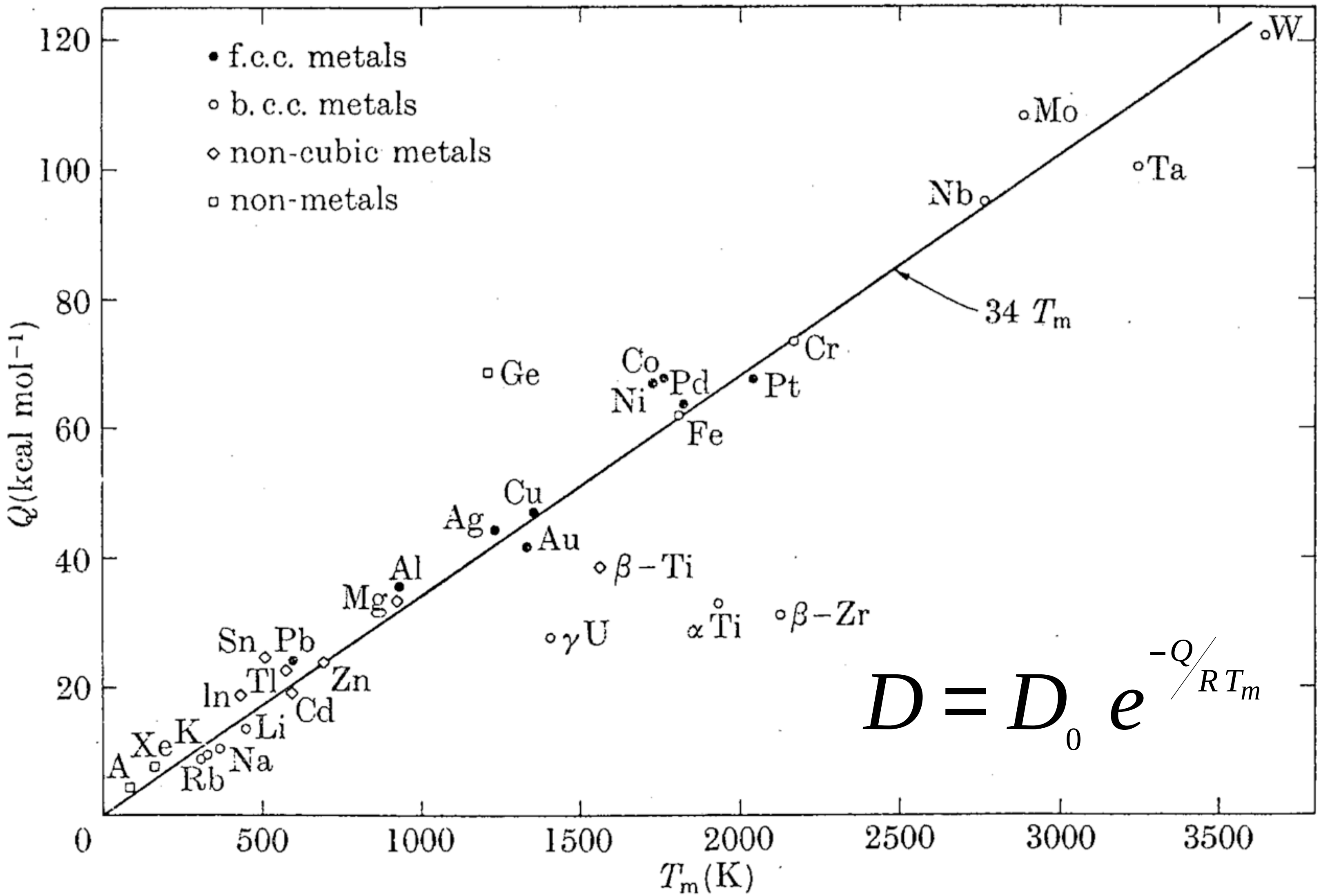

FIG. 14.31. The correlation between Q and T_m.

$$D = D_0 \, e^{-Q / R T_m}$$

C. Peter Flynn, *Point Defects and Diffusion* (Oxford, 1972) pp. 783-785.

Determining Surface Diffusion from RHEED Oscillations

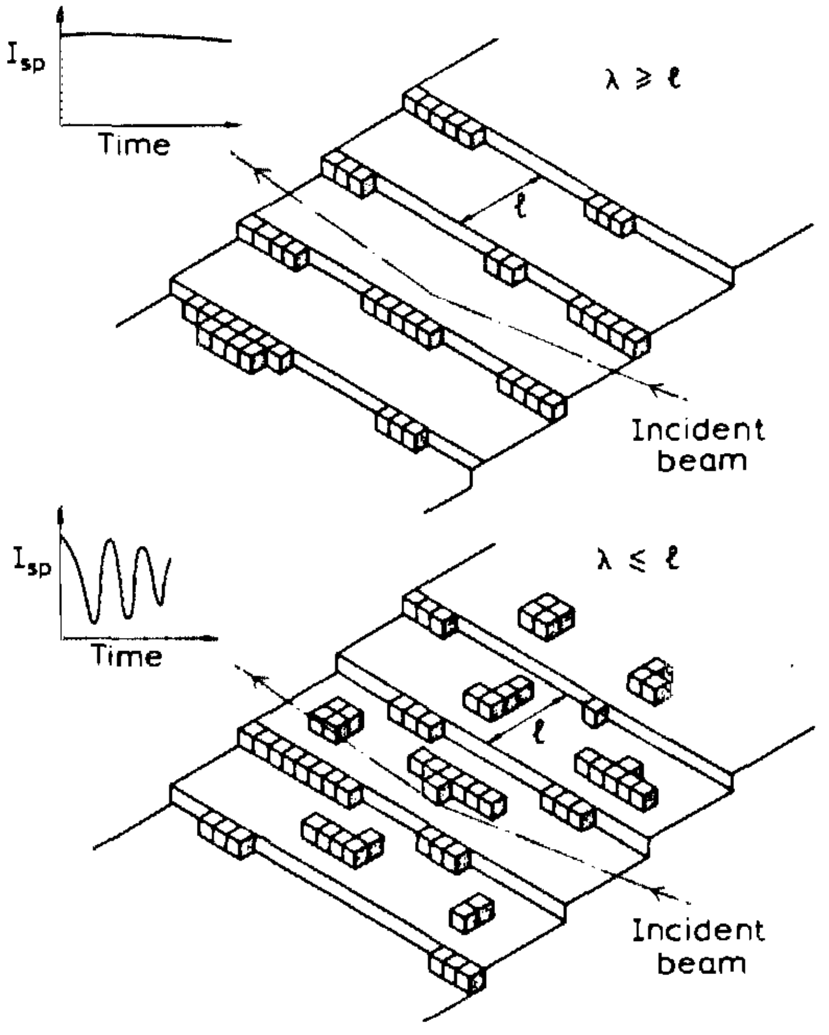

FIG. 1. Schematic illustration of the principle of the method, showing the change in RHEED information as the growth mode changes from "step flow" to 2-D nucleation. Steps lie along [100].

J.H. Neave, P.J. Dobson, B.A. Joyce, and J. Zhang, *Applied Physics Letters* **47** (1985) 100-102.

Surface vs. Bulk Diffusion

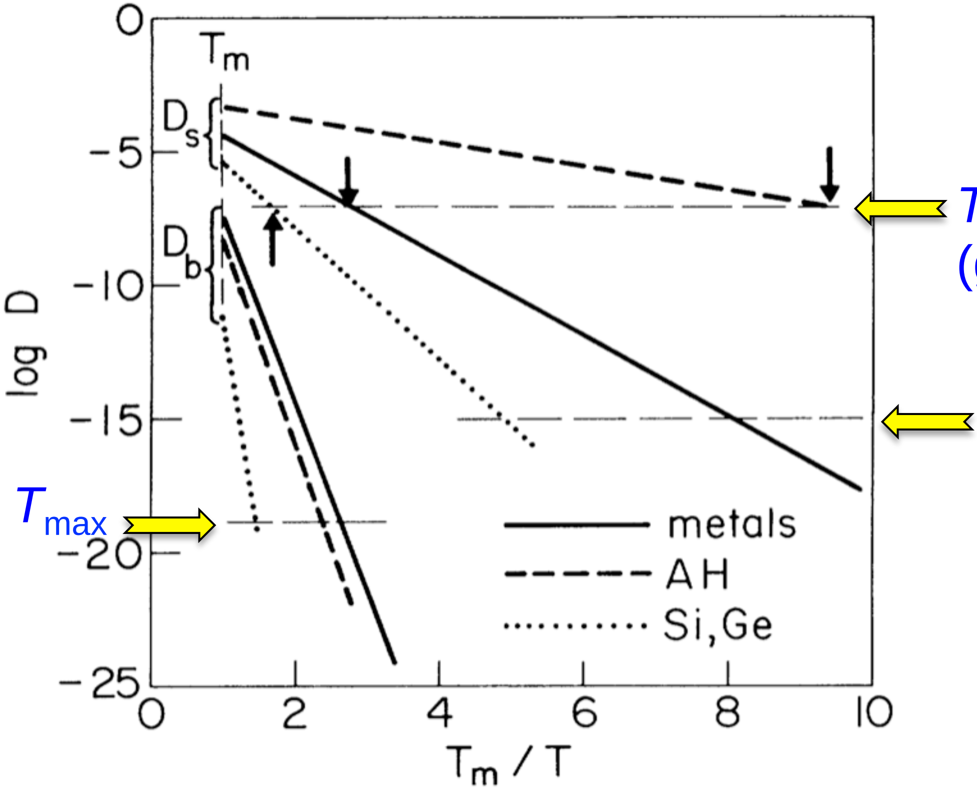

FIG. 6. Diagram showing deduced global dependences of surface and bulk diffusion coefficients, D_s and D_b, on T_m/T for metals (solid lines), elemental semiconductors (dotted lines), and salts (dashed lines). The construction is described in the text. Smooth flat interfaces generally require $D_s \gtrsim 10^{-8}$–10^{-7} cm^2/sec, which fixes the lowest growth temperatures (arrows) as $\sim 3T_m/8$, $0.55T_m$, and $0.1T_m$ in the three cases. RHEED oscillations are expected for $D_s \gtrsim 10^{-15}$ cm^2/sec and bulk interdiffusion for $D_b \gtrsim 10^{-19}$ cm^2/sec.

Assuming growth rate of 0.1 monolayer/sec

Optimal Growth Temperatures

$$0.55 < \frac{T_{sub}}{T_{melt}} < 0.7 \text{ for semiconductors}$$

$$0.35 < \frac{T_{sub}}{T_{melt}} < 0.4 \text{ for metals}$$

$$0.1 < \frac{T_{sub}}{T_{melt}} < 0.4 \text{ for simple ceramics}$$

M.H. Yang and C.P. Flynn, *Physical Review Letters* **62** (1989) 2476-2479.

Surface Energy Considerations

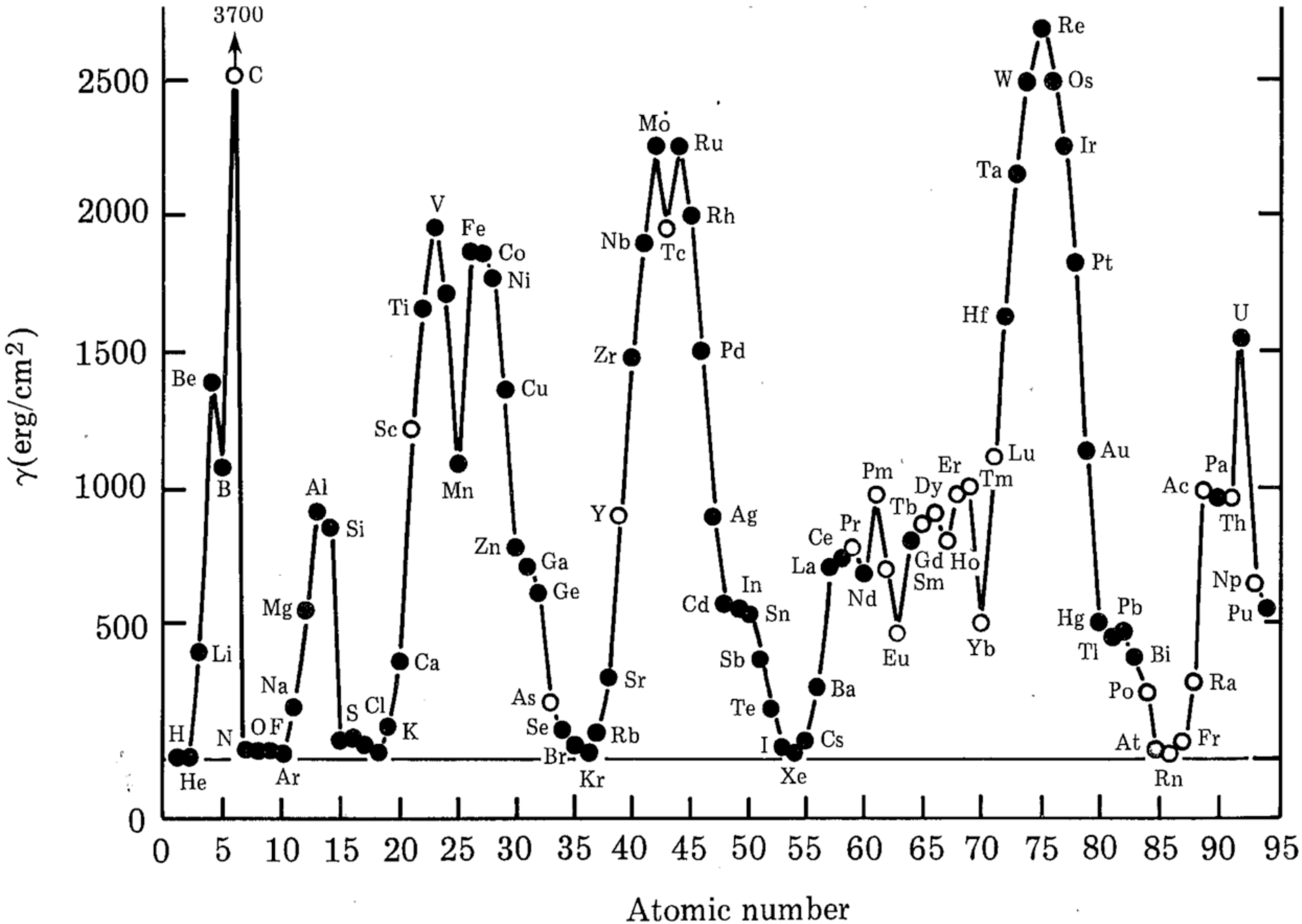

FIGURE 2.7 Surface tension of elements in the liquid phase (from Zangwill, 1988).

K.-N. Tu, J.W. Mayer, and L.C. Feldman,
Electronic Thin Film Science for Electrical Engineers and Materials Scientists (Macmillan, 1992).

Thermodynamic Considerations

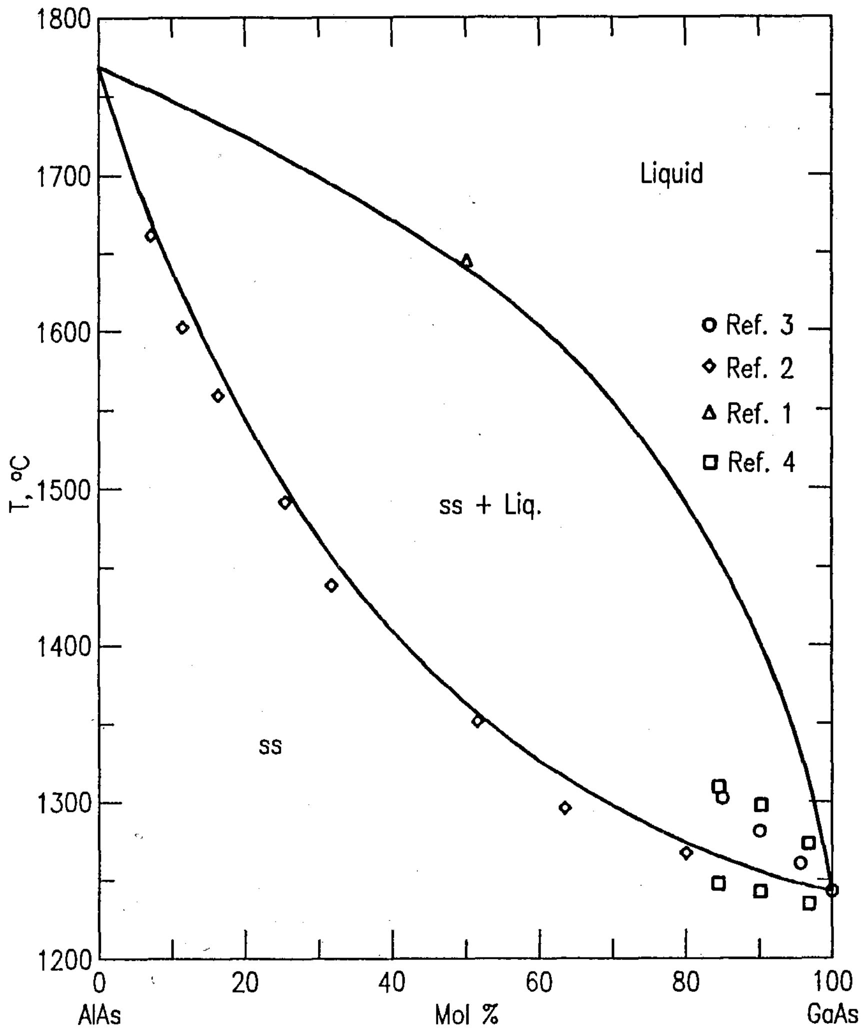

Fig. 8343—Pseudobinary system AlAs-GaAs.
K. Y. Ma, S. H. Li, and G. B. Stringfellow, "P, As, and Sb Phase Diagrams", Special Report to the Standard Reference Data Program, National Institute of Standards and Technology; Gaithersburg, Maryland (1987).

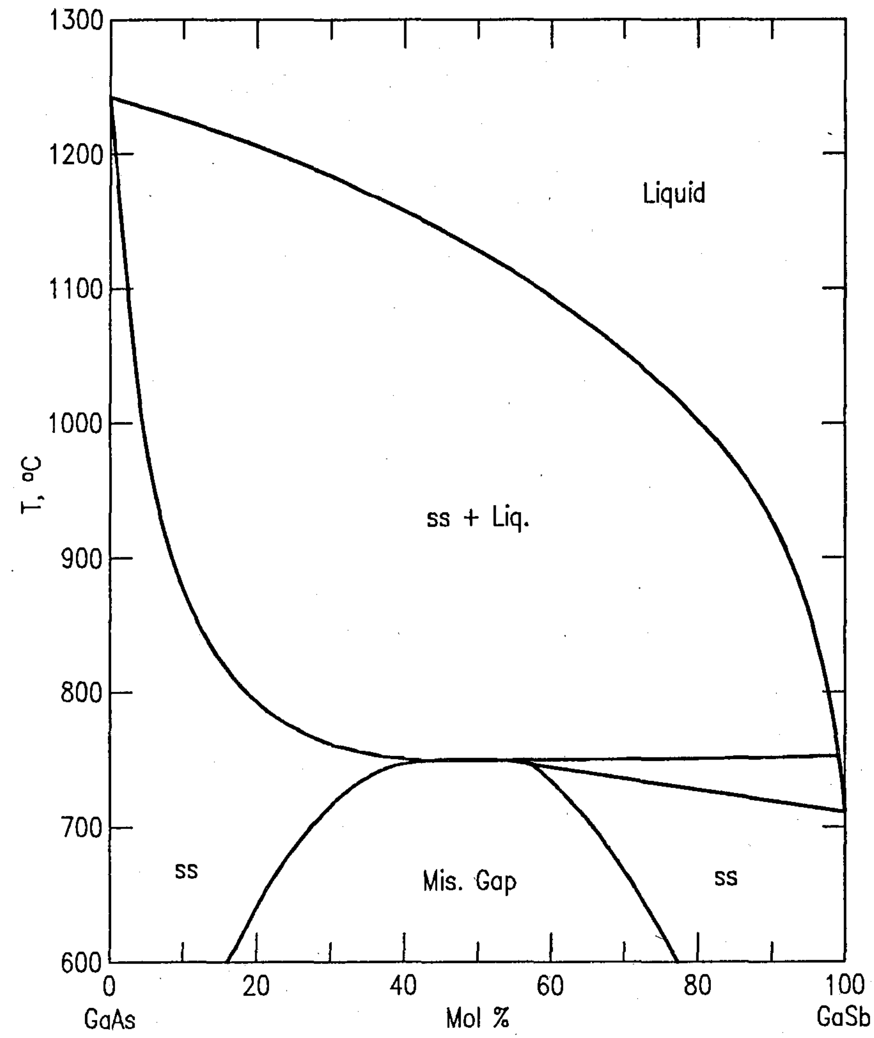

Fig. 8362—Pseudobinary system GaAs-GaSb. Calculated diagram.
K. Y. Ma, S. H. Li, and G. B. Stringfellow, "P, As, and Sb Phase Diagrams", Special Report to the Standard Reference Data Program, National Institute of Standards and Technology; Gaithersburg, Maryland (1987).

TEM of MBE-Grown Superlattices

AlAs / GaAs

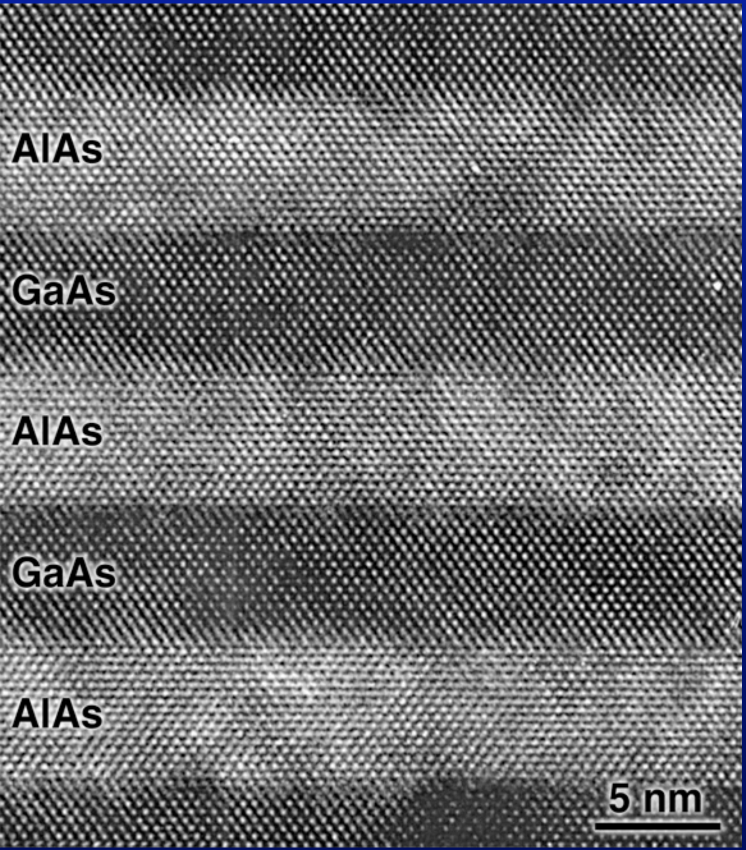

$PbTiO_3$ / $SrTiO_3$

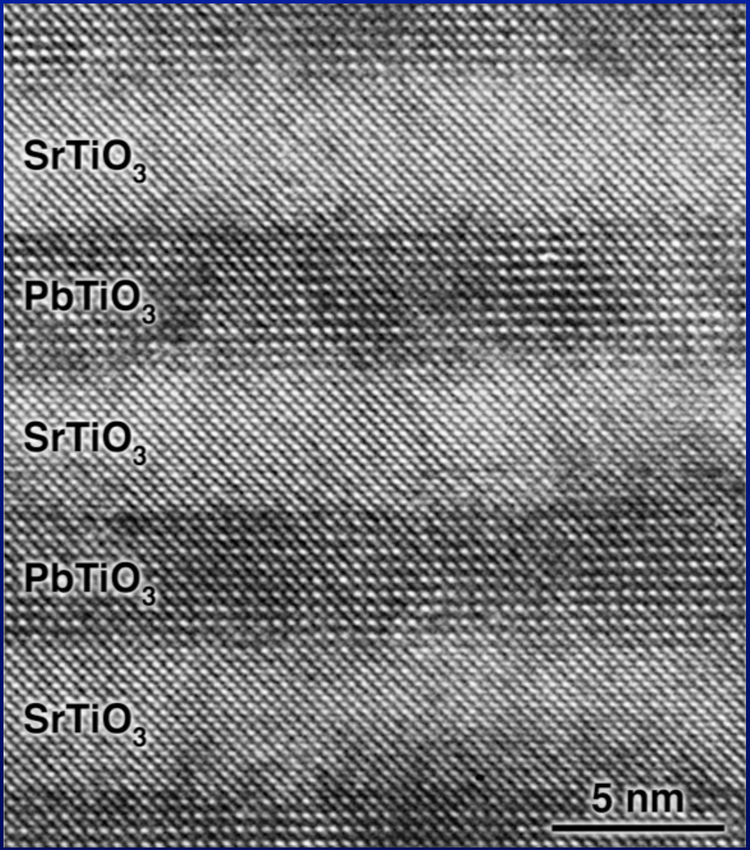

$BaTiO_3$ / $SrTiO_3$

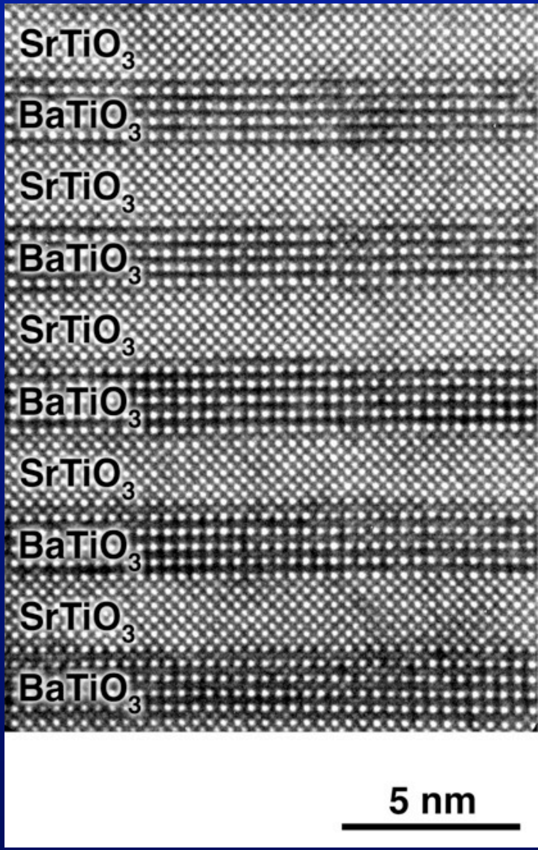

A.K. Gutakovskii *et al.*,
Phys. Stat. Sol. (a) **150** (1995) 127.

C.D. Theis
(1st Generation Schlom Group)

J.H. Haeni
(2nd Generation)

HRTEM—Pan Group (Michigan)

D.G. Schlom *et al.*, Mater. Sci. Eng. B **87** (2001) 282.

From the observed morphology, which likely has the higher surface energy?

(a) GaAs

(b) AlAs

(c) They appear to have the same surface energies

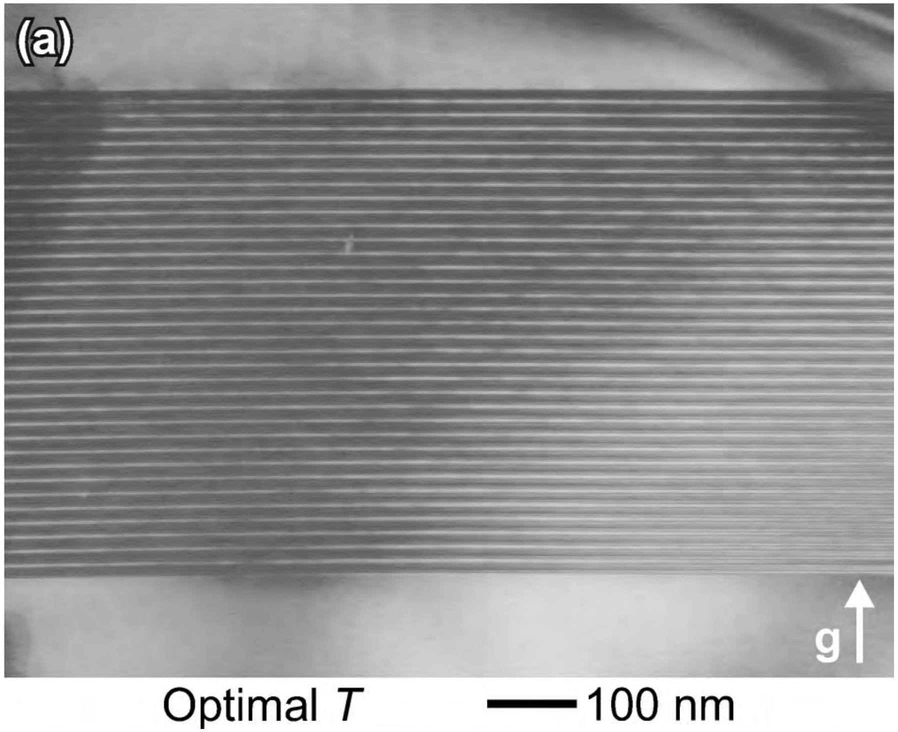

Increased Interface Roughness and Clustering at Non-Optimal Growth Conditions

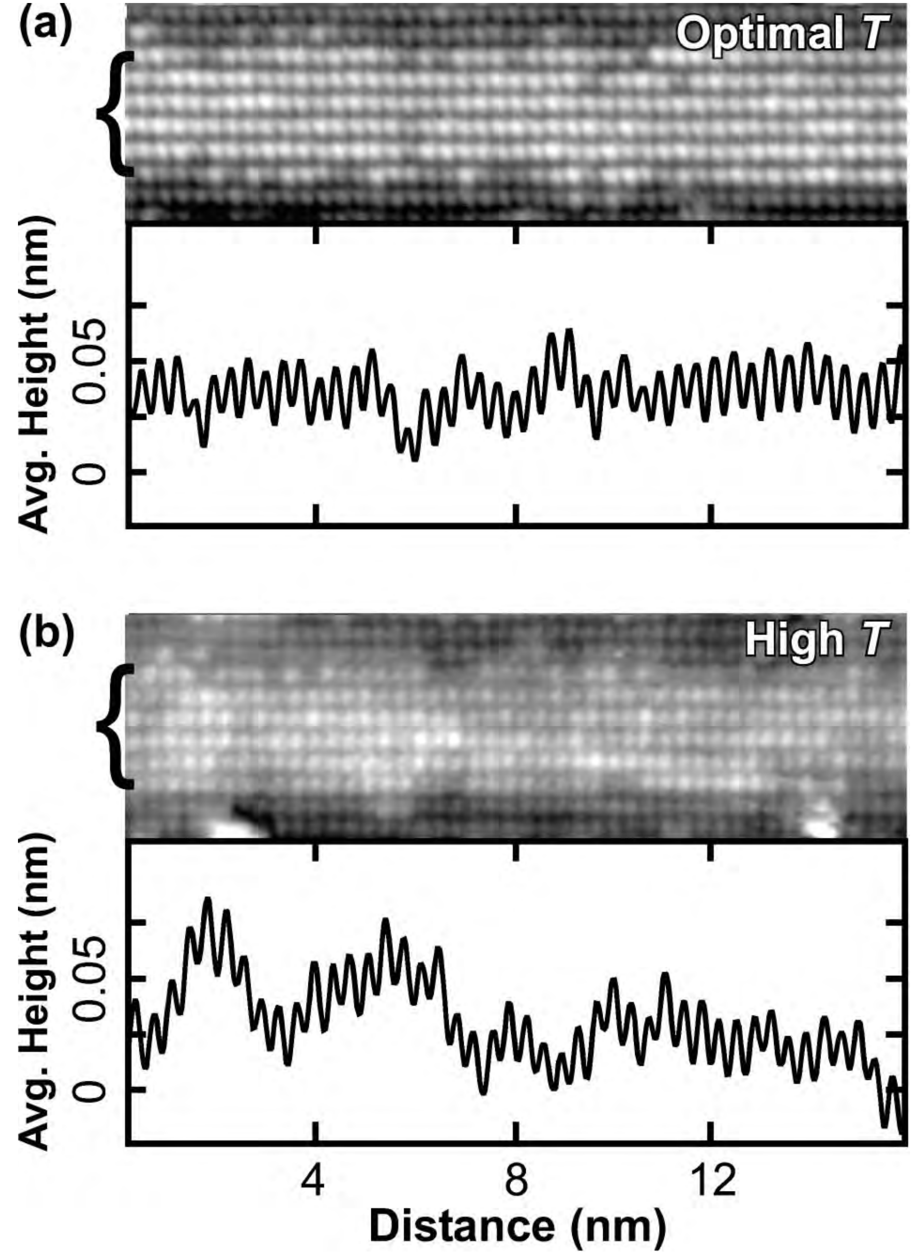

FIG. 6. XSTM images and average-height profiles for InGaSb-alloy layers in an (a) optimal- and (b) high-temperature sample. (a) −2.0 V, 50 pA and (b) −2.5 V, 0.5 nA.

W. Barvosa-Carter, M.E. Twigg, M.J. Yang, and L.J. Whitman, *Physical Review B* **63** (2001) 245311.

Nuts and Bolts of Oxide MBE

- Mean Free Path (maximum P_{O_2})
- Minimum P_{O_2}, need for P_{O_3}, Optimal T_{sub}
- MBE System, Sources, and Crucibles
- Composition Control
  - Adsorption-Controlled Growth
  - Flux-Controlled Growth
- Substrates

Oxide MBE System

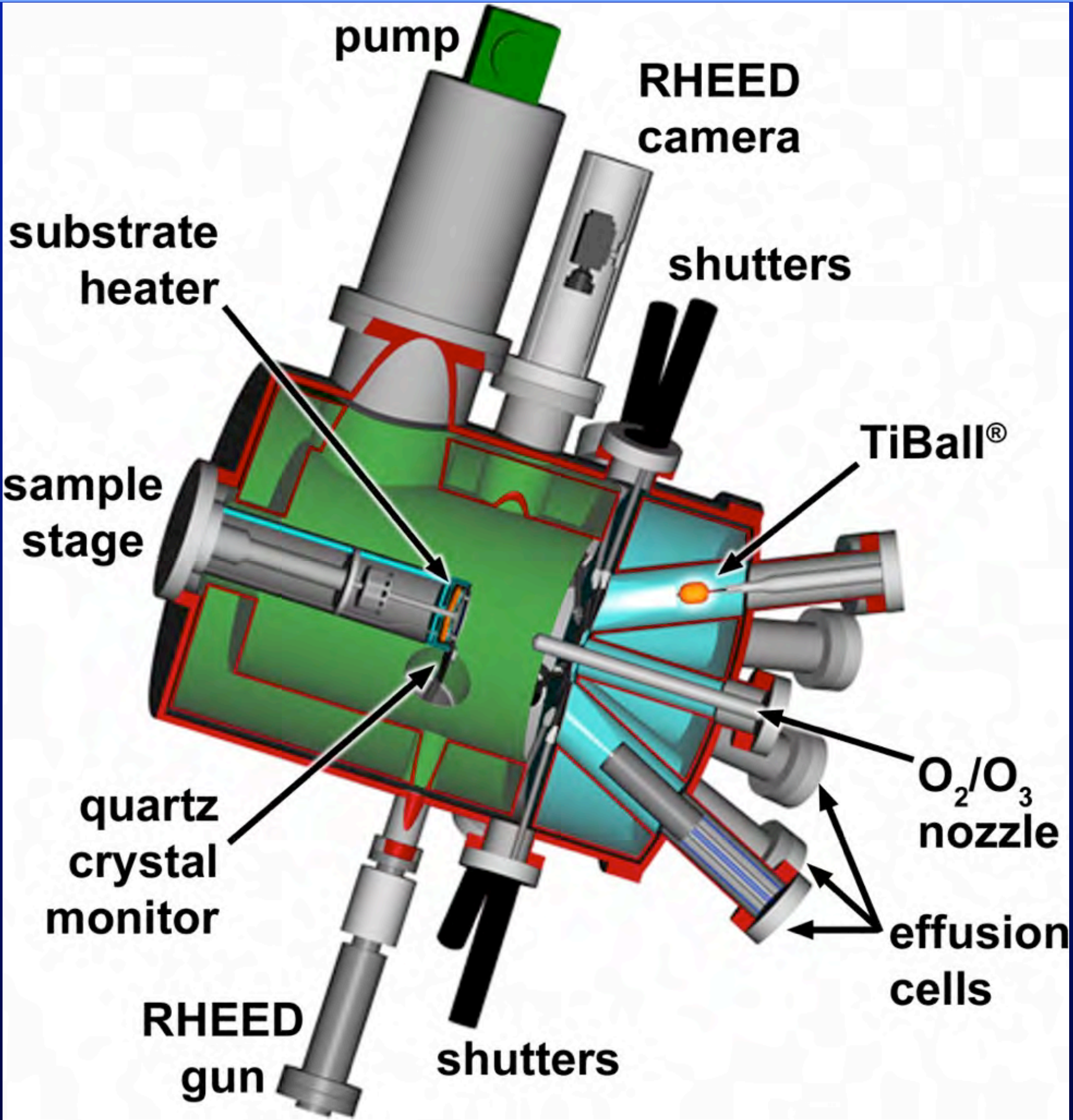

Oxide MBE at Brookhaven Nat. Lab.

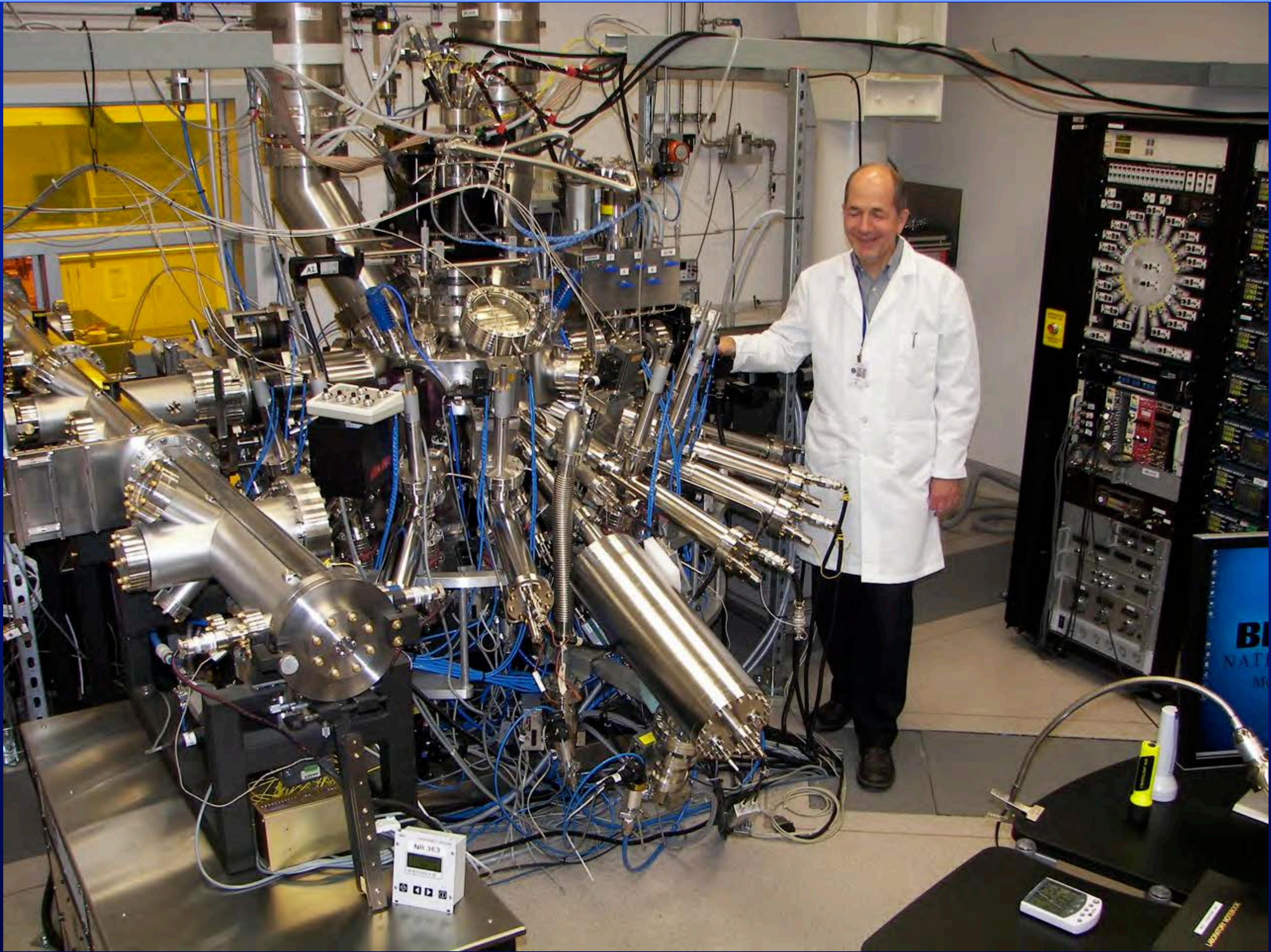

Oxide MBE + ARPES

Collaboration with Kyle Shen (Cornell, Physics)

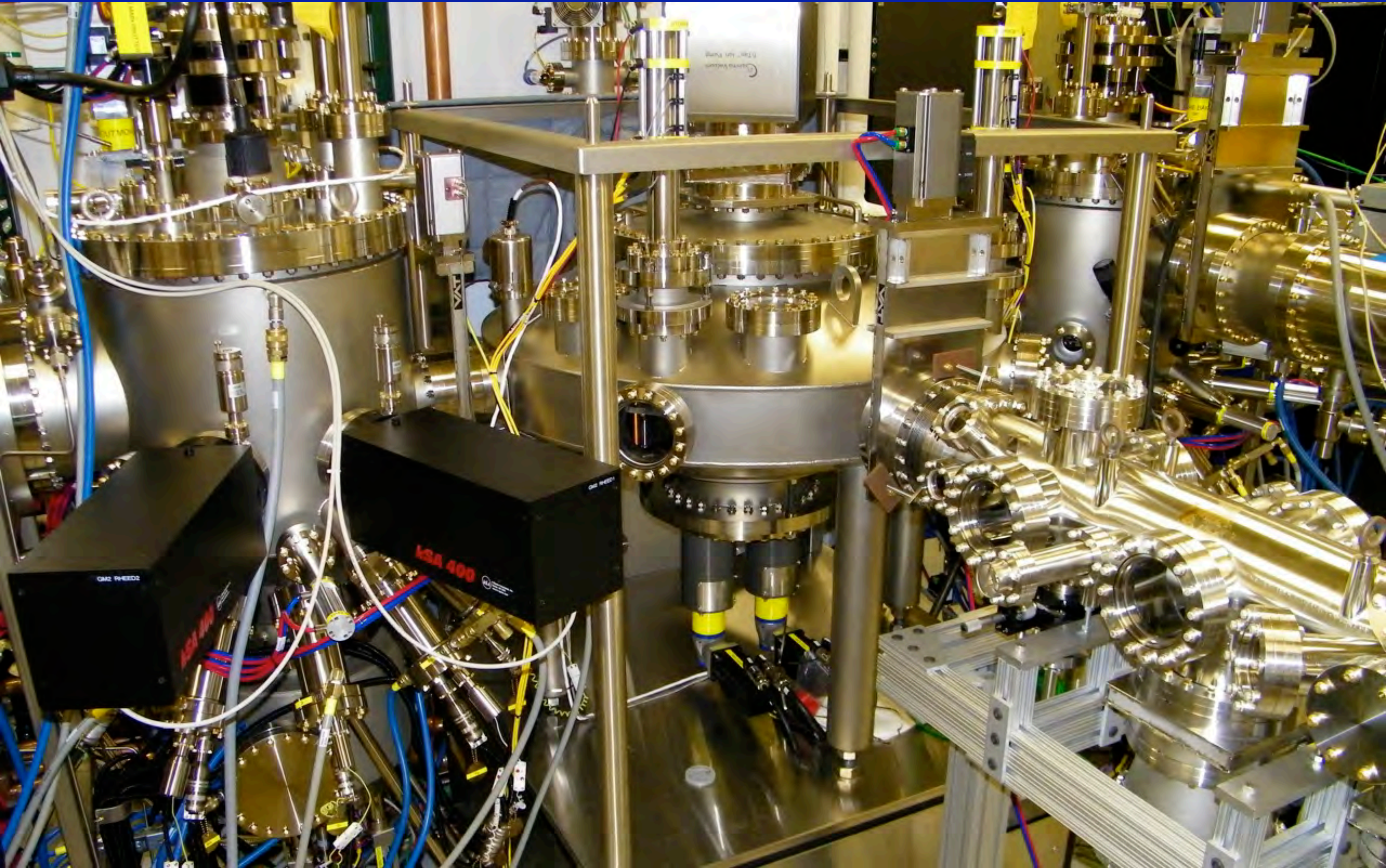

Automated Veeco GEN10 Oxide MBE

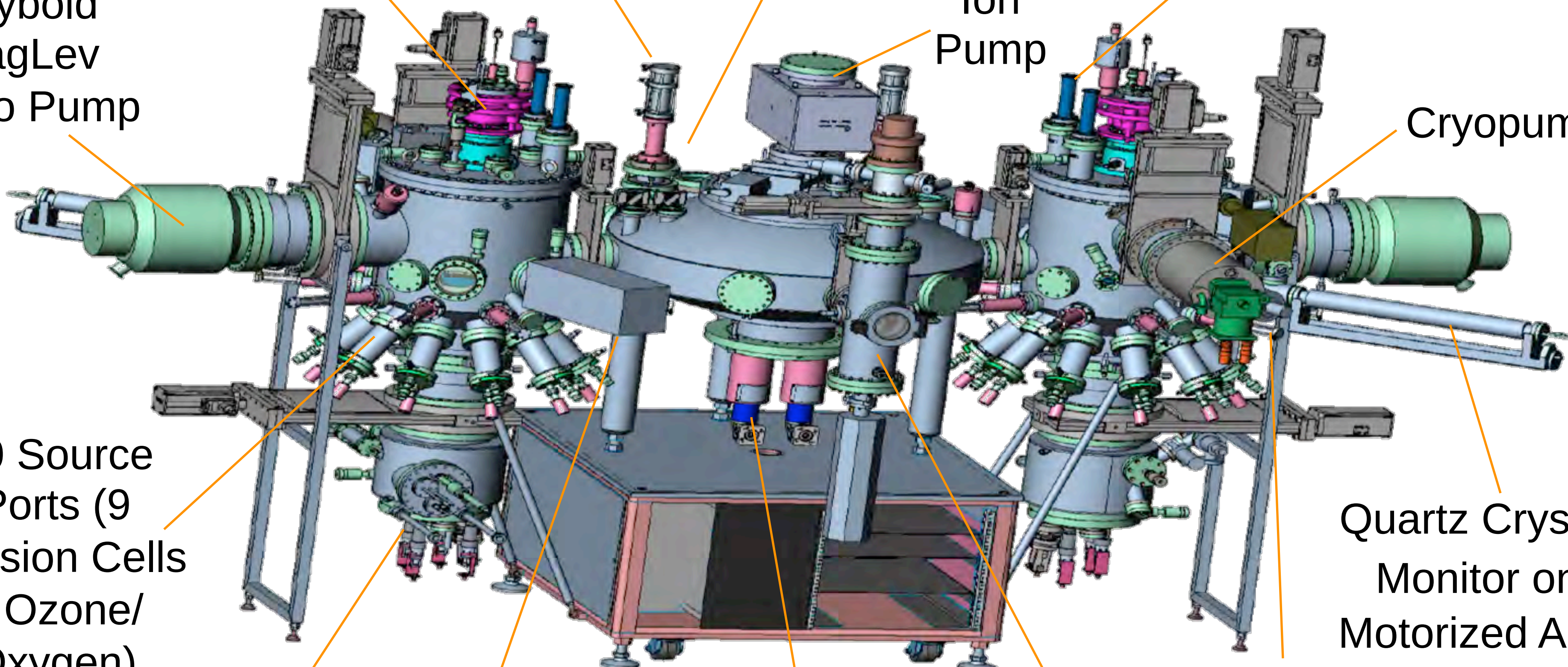

Sources for Oxide MBE

- **Effusion cell**
  (resistively heated thermal evaporators, up to 2000 °C), material in crucible

- **Ti-ball source**
  titanium sphere with resistive heater inside

- **e-gun evaporator**
  for extremely low vapor pressure materials (W, Ru, etc.)

Effusion Cell Temperatures

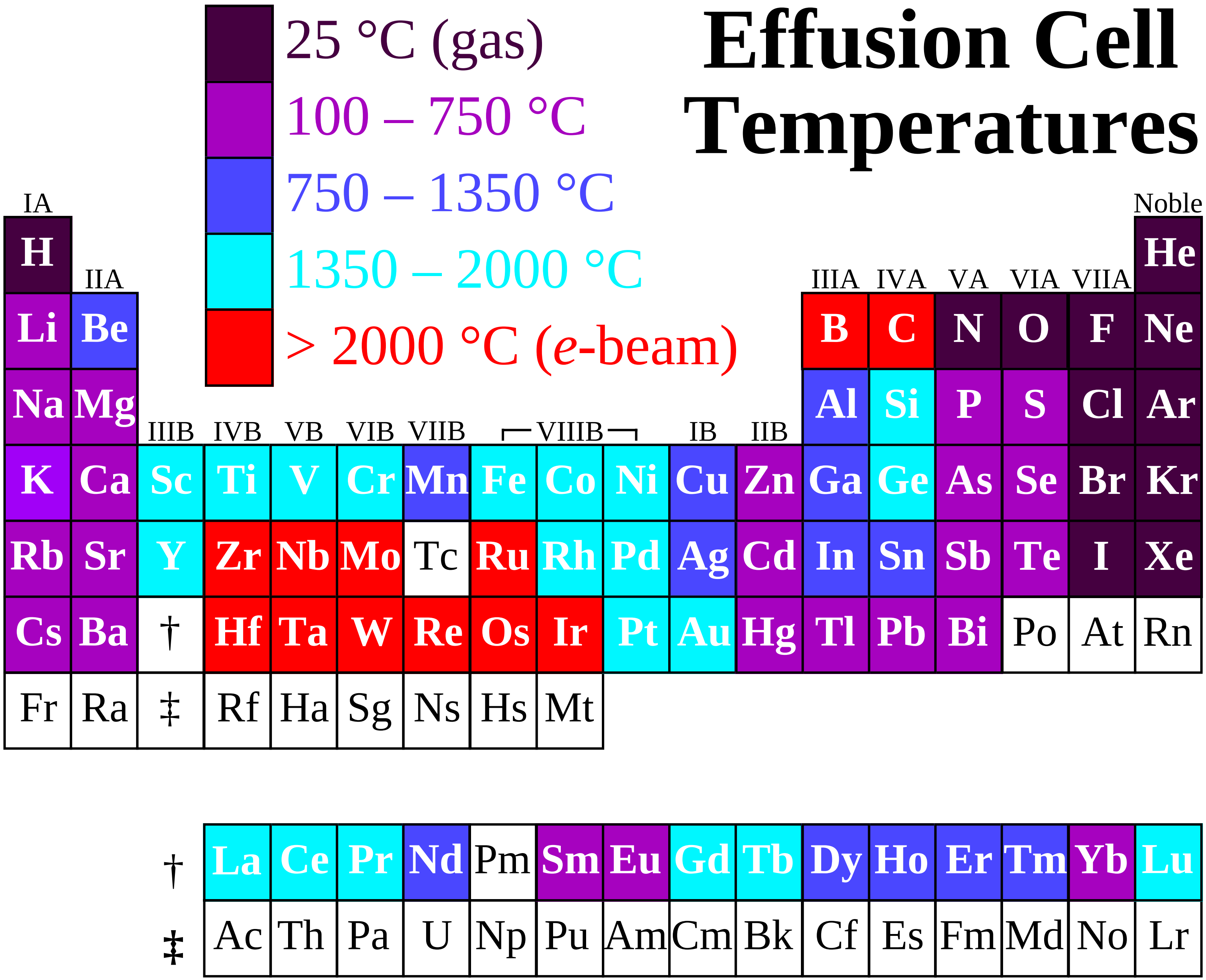

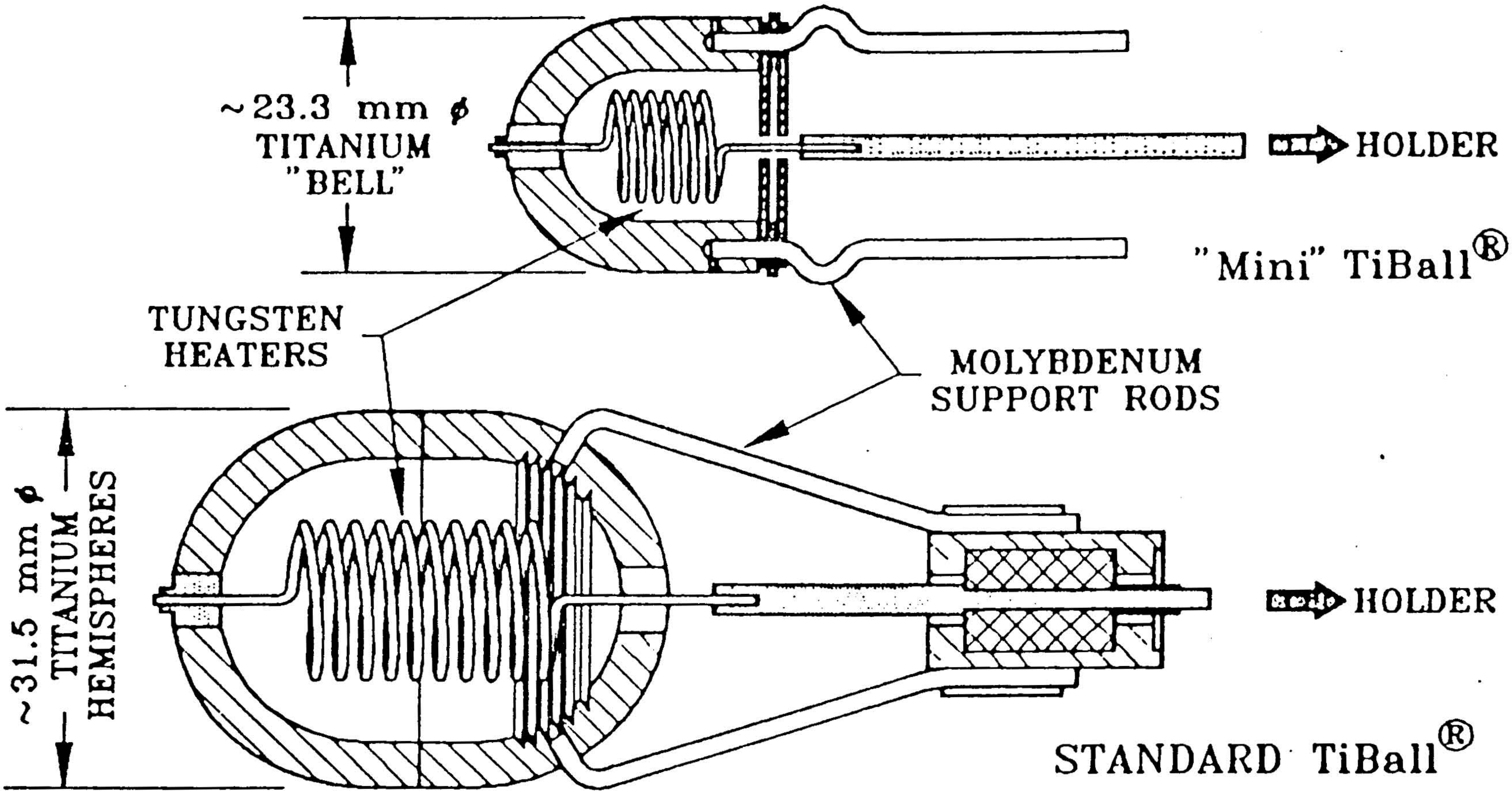

Figure 3.4.4. Two varieties of radiantly heated sublimation sources; the TiBall®, developed by Harra and Snouse(42) and a smaller, radiantly heated source developed by Welch.

CAPTURE PUMPING TECHNOLOGY

An Introduction

KIMO M. WELCH
Brookhaven National Laboratory, Upton, NY, USA

MBE Effusion Cells

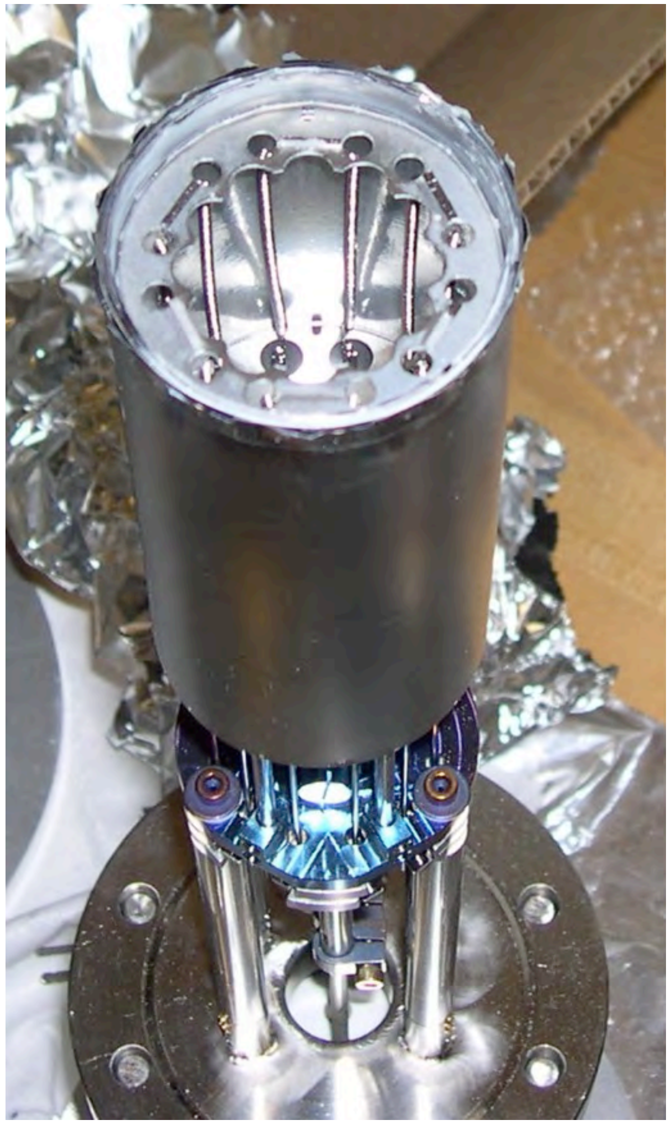

Arrhenius Plot of Vapor Pressure

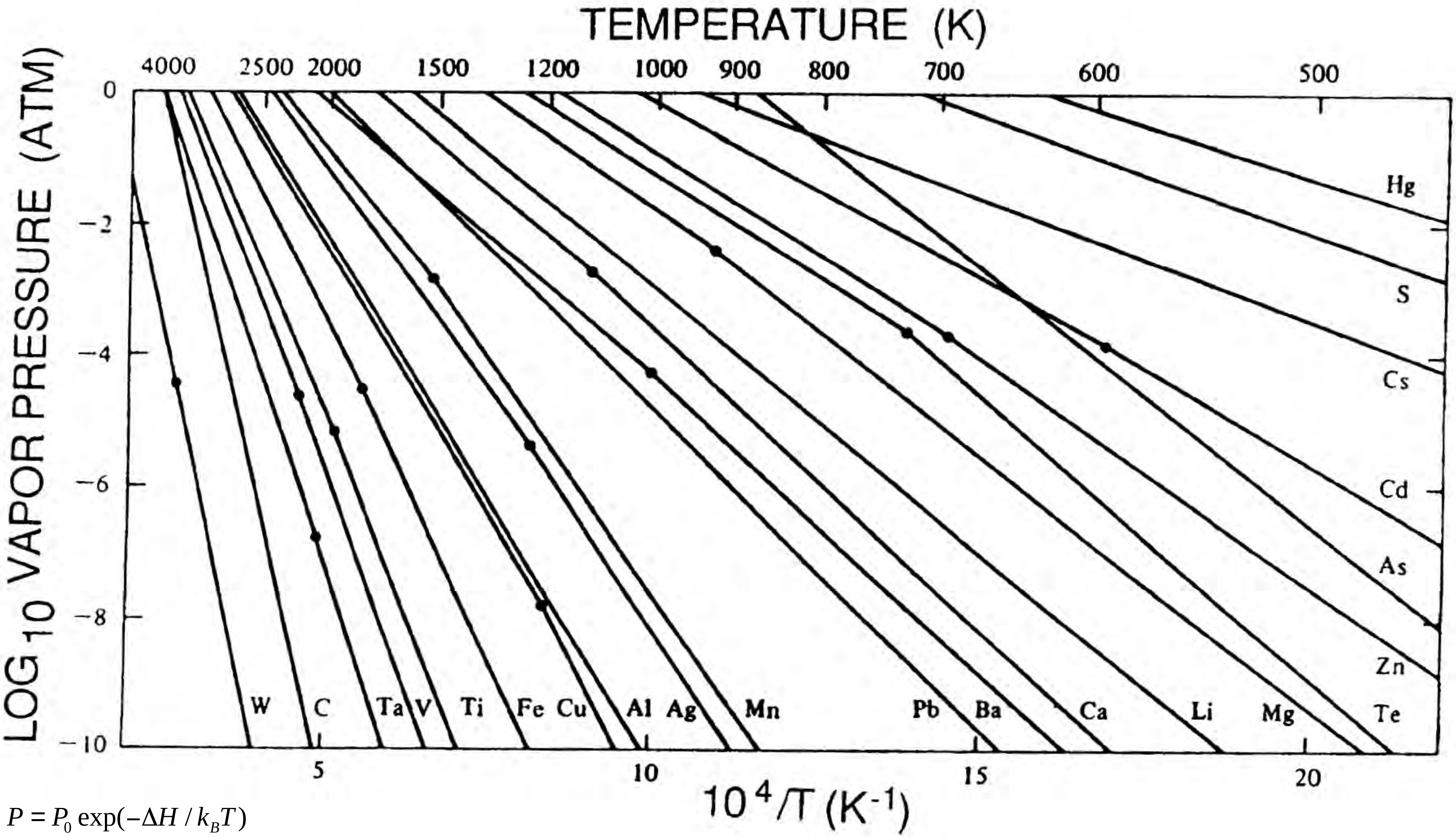

$$P = P_0 \exp(-\Delta H / k_B T)$$

$$\ln P = \ln P_0 - \left(\frac{\Delta H}{k_B}\right)\cdot\left(\frac{1}{T}\right)$$

so plot log(P) vs 1/T : straight line if ΔH is constant

(note small or no change in slope at melting point)

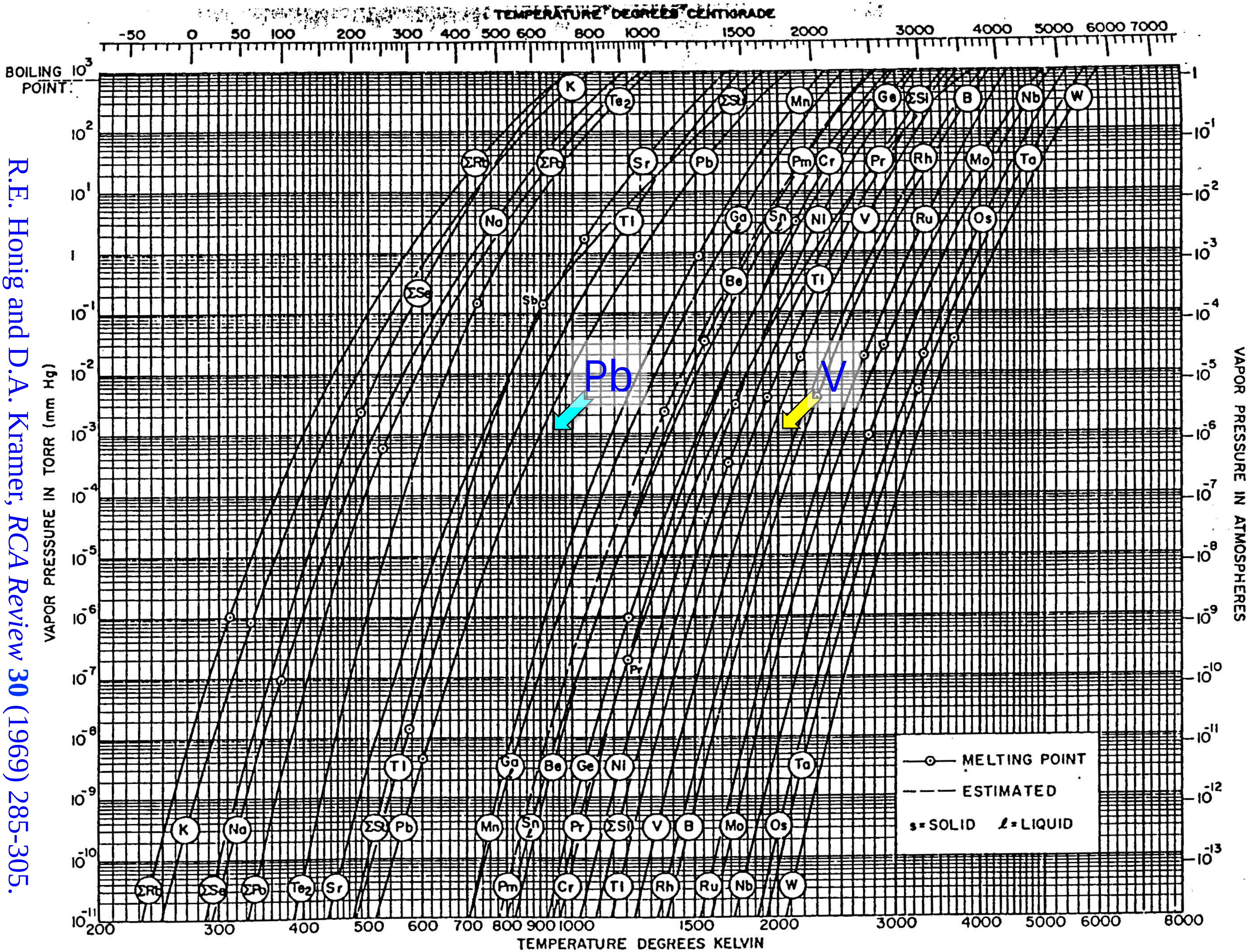

Fig. 1B—Vapor pressure data for the solid and liquid elements.

R.E. Honig and D.A. Kramer, *RCA Review* **30** (1969) 285-305.

Ti-Pb Phase Diagram

Binary Alloy Phase Diagrams,
edited by T.B. Massalski (ASM International, 1990).

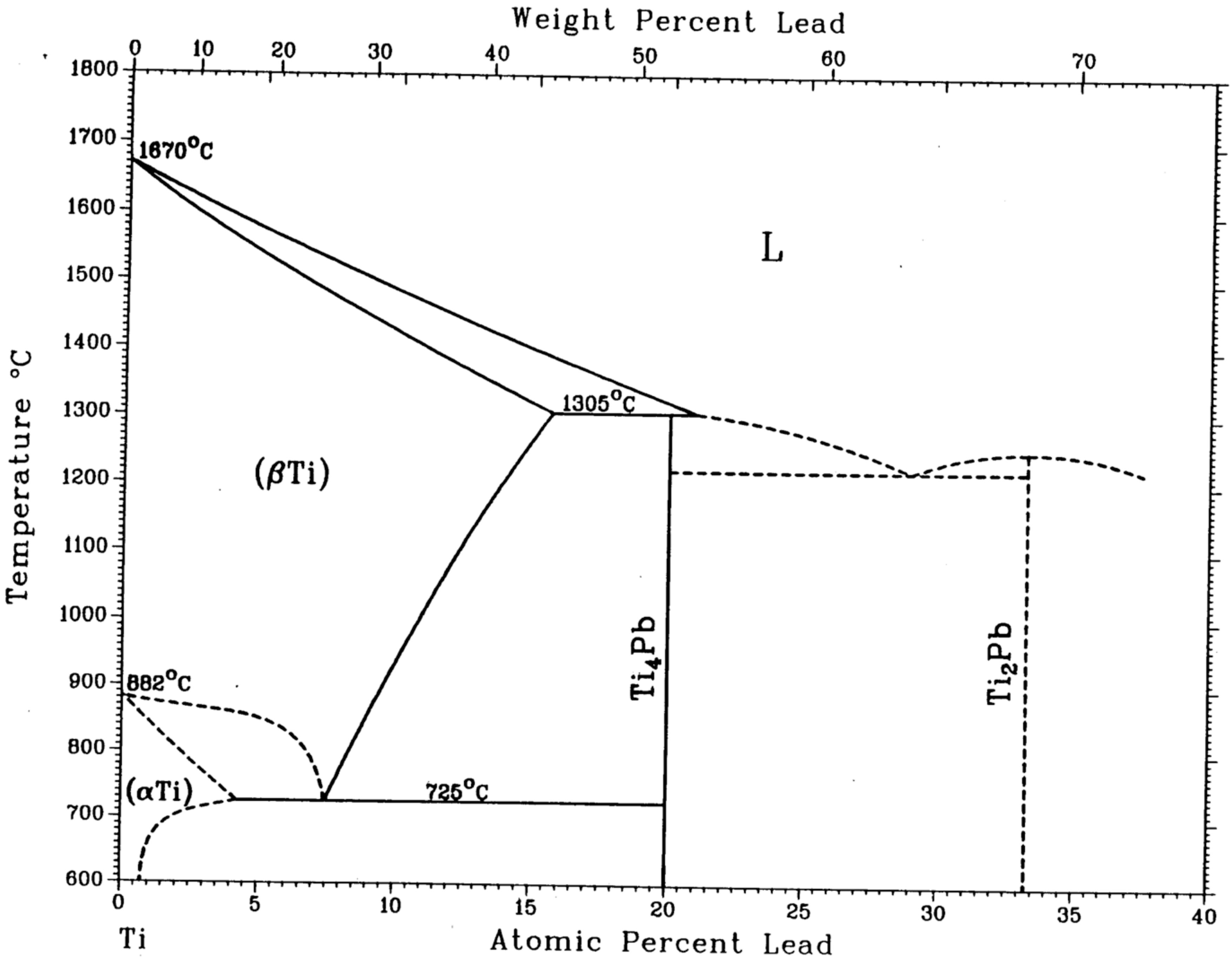

Mo-Pb Phase Diagram

Binary Alloy Phase Diagrams, edited by T.B. Massalski (ASM International, 1990).

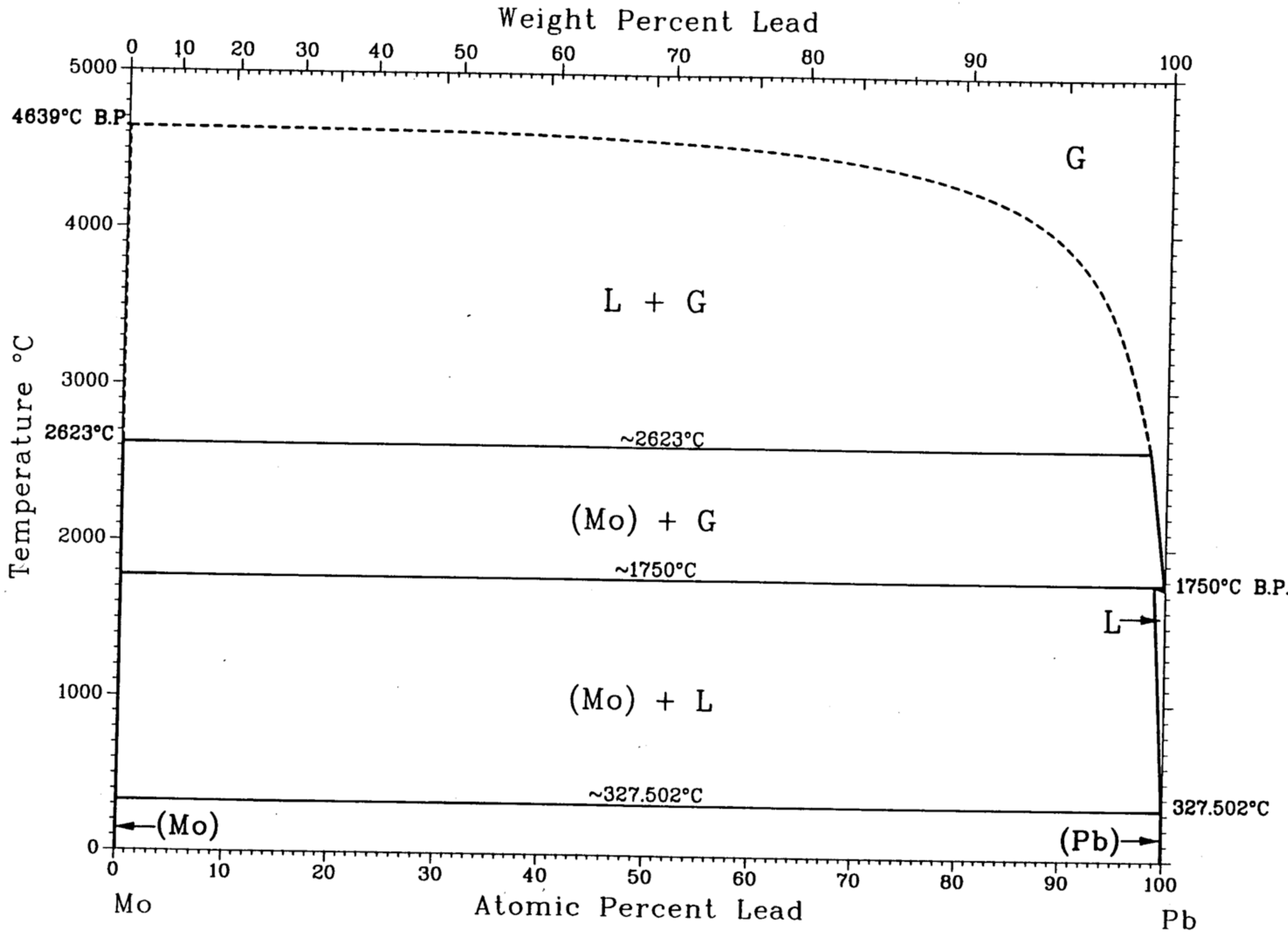

Binary Alloy Phase Diagrams,
edited by T.B. Massalski (ASM International, 1990).

Pb-W (Lead-Tungsten)

S.V. Nagender Naidu and P. Rama Rao

No phase diagram is available for the Pb-W system. The solubility of W in liquid Pb is less than 0.1 at.% W. No intermediate phases exist in the system.

[19Ino] clained to have determined the solidification temperature of alloys containing up to 30 at.% W at 1300 °C; however, no further details are available in this regard. The findings of [19Ino] are not accepted here because there is no confirming evidence in any of the later experimental investigations as to the alloy formation.

Pb-W Crystal Structure Data

Phase	Composition, at.% W	Pearson symbol	Space group	Strukturbericht designation	Prototype
(Pb)	~0	*cF*4	*Fm*$\bar{3}$*m*	*A*1	Cu
(W)	~100	*cI*2	*Im*$\bar{3}$*m*	*A*2	W

19Ino: S. Inouye, *Mem. Coll. Sci. Kyoto Univ.*, *4*, 43-46 (1919) in German.

To be published in *Phase Diagrams of Binary Tungsten Alloys*, 1991. Complete evaluation contains 1 table and 11 references.

What crucible would you use for Pb in MBE?

(a) Ti

(b) Mo

(c) W

Material	Symbol	MP (° C)	S/D	g/cm³	Temp. (° C) for Given Vap. Press. (Torr)			Evaporation Techniques					Sputter	Comments
					10^{-8}	10^{-6}	10^{-4}	E-Beam	Thermal Sources: Boat	Coil	Basket	Crucible		
Kanthal	FeCrAl	—	—	7.1	—	—	—	—	W	W	W	—	DC, RF	—
Lanthanum	La	921	—	6.15	990	1,212	1,388	Ex	W, Ta	—	—	Al_2O_3	RF	Films will burn in air if scraped
Lanthanum Boride	LaB_6	2,210	D	2.61	—	—	—	G	—	—	—	—	RF	—
Lanthanum Bromide	$LaBr_3$	783	—	5.06	—	—	—	—	—	—	Ta	—	RF	n=1.94. Hygroscopic
Lanthanum Fluoride	LaF_3	1,490	S	~6.0	—	—	900	G	Ta, Mo	—	Ta	—	RF	No decomposition. n ~1.6
Lanthanum Oxide	La_2O_3	2,307	—	6.51	—	—	1,400	G	W, Ta	—	—	—	RF	Loses oxygen. n~1.73
Lead	Pb	328	—	11.34	342	427	497	Ex	W, Mo	W	W, Ta	Al203, Q	DC,	RF Toxic
Lead Bromide	$PbBr_2$	373	—	6.66	—	—	~300	—	—	—	—	—	—	—
Lead Chloride	$PbCl_2$	501	—	5.85	—	—	~325	—	Pt	—	—	Al_2O_3	RF	Little decomposition
Lead Fluoride	PbF_2	855	S	8.24	—	—	~400	—	W, Pt, Mo	—	—	BeO	RF	n = 1.75
Lead Iodide	PbI_2	402	—	6.16	—	—	~500	—	Pt	—	—	Q	—	—
Lead Oxide	PbO	886	—	9.53	—	—	~550	—	Pt	—	—	Q, Al_2O_3	RF-R	No decomposition. n ~2.6
Lead Selenide	PbSe	1,065	S	8.10	—	—	~500	—	W, Mo	—	W	Gr, Al_2O_3	RF	—
Lead Stannate	$PbSnO_3$	1,115	—	8.1	670	780	905	P	Pt	—	Pt	Al_2O_3	RF	Disproportionates
Lead Sulfide	PbS	1,114	S	7.5	—	—	500	—	W	—	W, Mo	Q, Al_2O_3	RF	Little decomposition. n = 3.92
Lead Telluride	PbTe	917	—	8.16	780	910	1,050	—	Mo, Pt, Ta	—	—	Al_2O_3, Gr	RF	Vapors toxic. Deposits aretellurium rich. Sputtering preferred or co-evaporate from two sources
Lead Titanate	$PbTiO_3$	—	—	7.52	—	—	—	—	Ta	—	—	—	RF	—
Lithium	Li	181	—	0.53	227	307	407	G	Ta, SS	—	—	Al_2O_3, BeO	—	Metal reacts quickly in air
Lithium Bromide	LiBr	550	—	3.46	—	—	~500	—	Ni	—	—	—	RF	n = 1.78
Lithium Chloride	LiCl	605	—	2.07	—	—	400	—	Ni	—	—	—	RF	Preheat gently to outgas. n = 1.66
Lithium Fluoride	LiF	845	—	2.64	875	1,020	1,180	G	Ni, Ta, Mo, W	—	—	Al_2O_3	RF	Rate control important for optical films. Preheat gently to outgas. n = 1.39
Lithium Iodide	LiI	449	—	4.08	—	—	400	—	Mo, W	—	—	—	RF	n = 1.96
Lithium Oxide	Li_2O	>1,700	—	2.01	—	—	850	—	Pt, Ir	—	—	—	RF	n = 1.64
Lutetium	Lu	1,663	—	9.84	—	—	1,300	Ex	Ta	—	—	Al_2O_3	RF, DC	—
Lutetium Oxide	Lu_2O_3	—	—	9.42	—	—	1,400	—	Ir	—	—	—	RF	Decomposes

Key of Symbols: * influenced by composition; ** Cr-plated rod or strip; ***all metals alumina coated; **C** = carbon; **Gr** = graphite; **Q** = quartz; **Incl** = Inconel; **VC** = vitreous carbon; **SS** = stainless steel; **Ex** = excellent; **G** = good; **F** = fair; **P** = poor; **S** = sublimes; **D** = decomposes; **RF** = RF sputtering is effective; **RF-R** = reactive RF sputter is effective; **DC** = DC sputtering is effective; **DC-R** = reactive DC sputtering is effective

Kurt J. Lesker, Co. Catalog

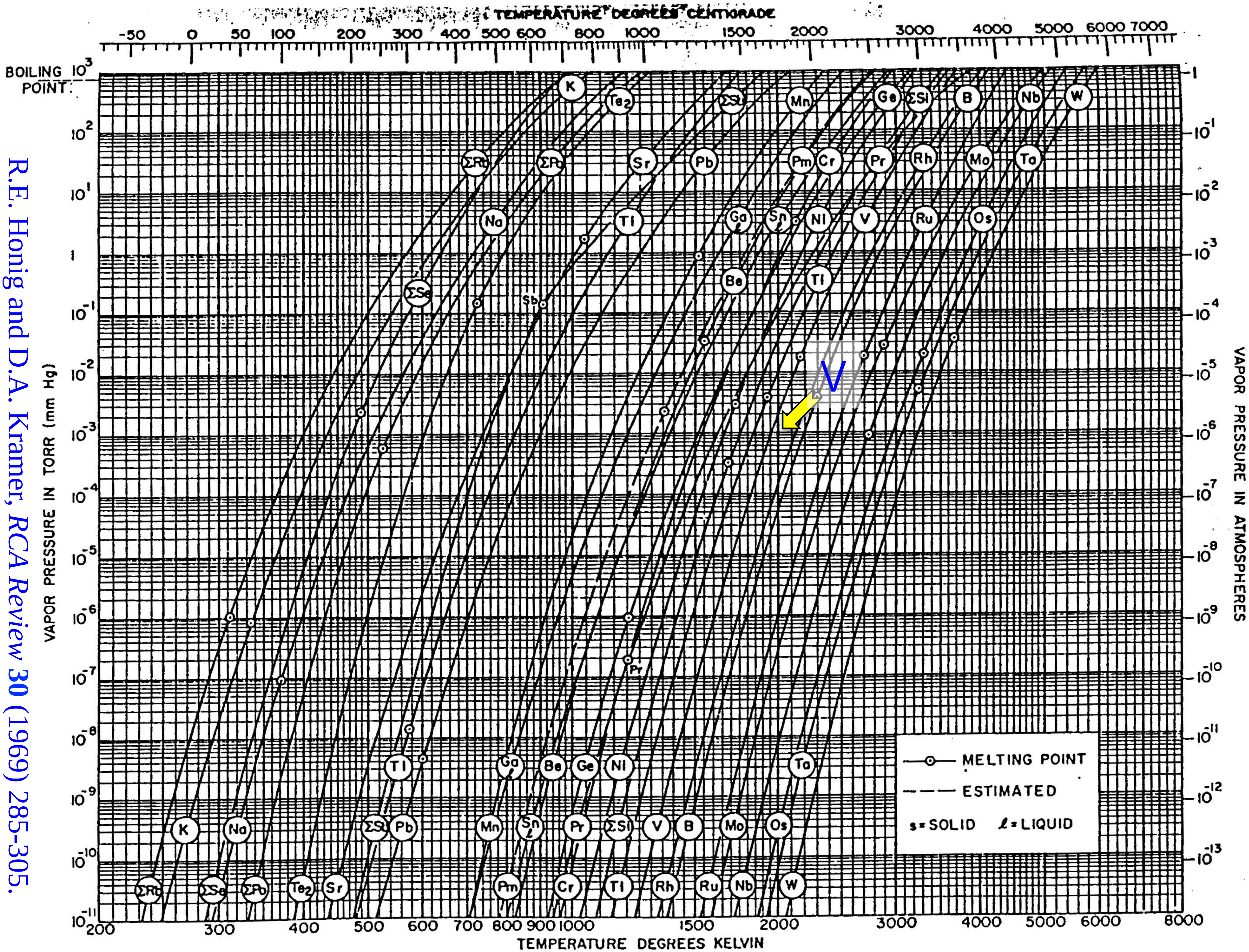

R.E. Honig and D.A. Kramer, *RCA Review* **30** (1969) 285-305.

Fig. 1B—Vapor pressure data for the solid and liquid elements.

Material	Symbol	MP (° C)	S/D	g/cm³	Temp. (° C) for Given Vap. Press. (Torr) 10^{-8}	10^{-6}	10^{-4}	Evaporation Techniques E-Beam	Thermal Sources Boat	Coil	Basket	Crucible	Sputter	Comments
Thulium	Tm	1,545	S	9.32	461	554	680	G	Ta	—	—	Al_2O_3	DC	—
Thulium Oxide	Tm_2O_3	—	—	8.90	—	—	1,500	—	Ir	—	—	—	RF	Decomposes
Tin	Sn	232	—	7.28	682	807	997	Ex	Mo	W	W	Al_2O_3	DC, RF	Wets molybdenum. Use tantalum liner in E-beam guns
Tin Oxide	SnO_2	1,630	S	6.95	—	—	~1,000	Ex	W	W	W	Q, Al_2O_3	RF, RF-R	Films from tungsten are oxygen deficient, oxidize in air. n = 2.0
Tin Selenide	SnSe	861	—	6.18	—	—	~400	G	—	—	—	Q	RF	—
Tin Sulfide	SnS	882	—	5.22	—	—	~450	—	—	—	—	Q	RF	—
Tin Telluride	SnTe	780	D	6.48	—	—	~450	—	—	—	—	Q	RF	—
Titanium	Ti	1,660	—	4.5	1,067	1,235	1,453	Ex	W	—	—	TiC	DC, RF	Alloys with refractory metals; evolves gas on first heating
Titanium Boride	TiB_2	2,900	—	4.50	—	—	—	P	—	—	—	—	RF, DC	—
Titanium Carbide	TiC	3,140	—	4.93	—	—	~2,300	—	—	—	—	—	RF, DC	—
Titanium Nitride	TiN	2,930	—	5.22	—	—	—	G	Mo	—	—	—	RF, RF-R, DC	Sputtering preferred. Decomposes with thermal evaporation
Titanium (II) Oxide	TiO	1,750	—	4.93	—	—	~1,500	G	W, Mo	—	—	VC	RF	Preheat gently to outgas. n = 2.2
Titanium (III) Oxide	Ti_2O_3	2,130	D	4.6	—	—	—	G	W	—	—	—	RF	Decomposes
Titanium (IV) Oxide	TiO_2	1,830	—	4.26	—	—	~1,300	F	W, Mo	—	W	—	RF, RF-R	Suboxide, must be reoxidized to rutile. Tantalum reduces TiO_2 to TiO and titanium. n = 2.616, 2.903
Tungsten	W	3,410	—	19.35	2,117	2,407	2,757	G	—	—	—	—	RF, DC	Forms volatile oxides. Films hard and adherent
Tungsten Boride	WB_2	~2,900	—	10.77	—	—	—	P	—	—	—	—	RF	—
Tungsten Carbide	W_2C	2,860	—	17.15	1,480	1,720	2,120	Ex	C	—	—	—	RF, DC	—
Tungsten Disulfide	WS_2	1,250	D	7.5	—	—	—	—	—	—	—	—	RF	—
Tungsten Oxide	WO_3	1,473	S	7.16	—	—	980	G	W, Pt	—	—	—	RF-R	Preheat gently to outgas. Tungsten reduces oxide slightly. n = 1.68
Tungsten Selenide	WSe_2	—	—	9.0	—	—	—	—	—	—	—	—	RF	—
Tungsten Silicide	WSi_2	>900	—	9.4	—	—	—	—	—	—	—	—	RF, DC	—
Tungsten Telluride	WTe_3	—	—	9.49	—	—	—	—	—	—	—	Q	RF	—
Uranium	U	1,132	—	19.05	1,132	1,327	1,582	G	Mo, W	W	W	—	—	Films oxidize
Uranium Carbide	UC_2	2,350	—	11.28	—	—	2,100	—	—	—	—	C	RF	Decomposes
Uranium Fluoride	UF_4	960	—	6.70	—	—	300	—	Ni	—	—	—	RF	—
Uranium (III) Oxide	U_2O_3	1,300	D	8.30	—	—	—	—	W	—	W	—	RF-R	Disproportionates at 1,300° C to UO_2
Uranium (IV) Oxide	UO_2	2,878	—	10.96	—	—	—	—	W	—	W	—	RF	Tantalum causes decomposition
Uranium Phosphide	UP_2	—	—	8.57	—	—	1,200	—	Ta	—	—	—	RF	Decomposes
Uranium (II) Sulfide	US	>2,000	—	10.87	—	—	—	—	—	—	—	—	—	—
Uranium (IV) Sulfide	US_2	>1,100	—	7.96	—	—	—	—	W	—	—	—	RF	Slight decomposition
Vanadium	V	1,890	—	5.96	1,162	1,332	1,547	Ex	W, Mo	—	—	—	DC, RF	Wets molybdenum. E-beam-evaporated films preferred. n = 3.03
Vanadium Boride	VB_2	2,400	—	5.10	—	—	—	—	—	—	—	—	RF, DC	—
Vanadium Carbide	VC	2,810	—	5.77	—	—	~1,800	—	—	—	—	—	RF, DC	—
Vanadium Nitride	VN	2,320	—	6.13	—	—	—	—	—	—	—	—	RF, RF-R, DC	—
Vanadium (IV) Oxide	VO_2	1,967	S	4.34	—	—	~575	—	—	—	—	—	RF, RF-R	Sputtering preferred.
Vanadium (V) Oxide	V_2O_5	690	D	3.36	—	—	~500	—	—	—	—	Q	RF	n = 1.46, 1.52, 1.76
Vanadium Silicide	VSi_2	1,700	—	4.42	—	—	—	—	—	—	—	—	RF	—
Ytterbium	Yb	819	S	6.96	520	590	690	G	Ta	—	—	—	DC, RF	—
Ytterbium Fluoride	YbF_3	1,157	—	—	—	—	~800	—	Mo	—	—	—	RF	—
Ytterbium Oxide	Yb_2O_3	2,346	S	9.17	—	—	~1,500	—	Ir	—	—	—	RF, RF-R	Loses oxygen

Key of Symbols: * influenced by composition; ** Cr-plated rod or strip; ***all metals alumina coated; **C** = carbon; **Gr** = graphite; **Q** = quartz; **Incl** = Inconel; **VC** = vitreous carbon; **SS** = stainless steel; **Ex** = excellent; **G** = good; **F** = fair; **P** = poor; **S** = sublimes; **D** = decomposes; **RF** = RF sputtering is effective; **RF-R** = reactive RF sputter is effective; **DC** = DC sputtering is effective; **DC-R** = reactive DC sputtering is effective

Kurt J. Lesker, Co. Catalog

C-V, Sr-V, Ti-V, and W-V Phase Diagrams

Desk Handbook: *Phase Diagrams for Binary Alloys*, edited by H. Okamoto (ASM International, 2000).

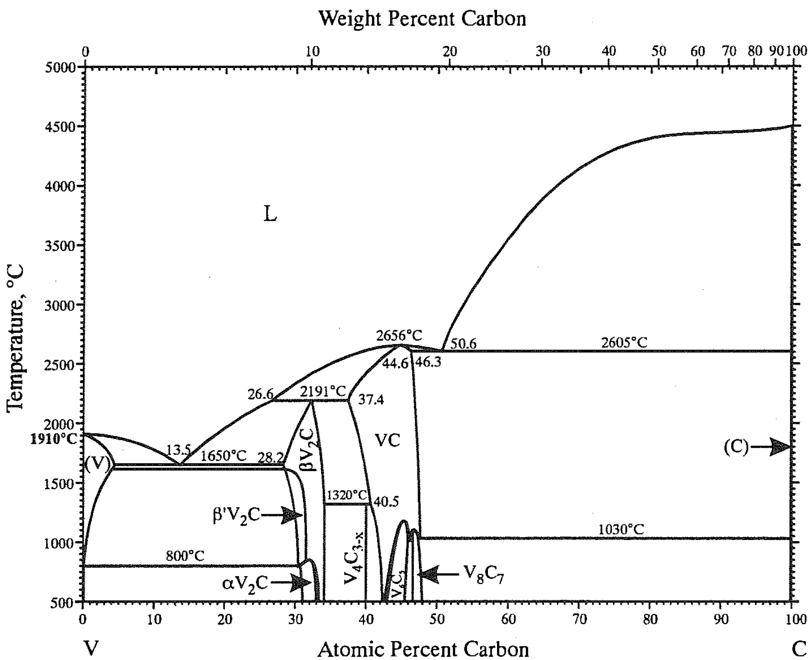

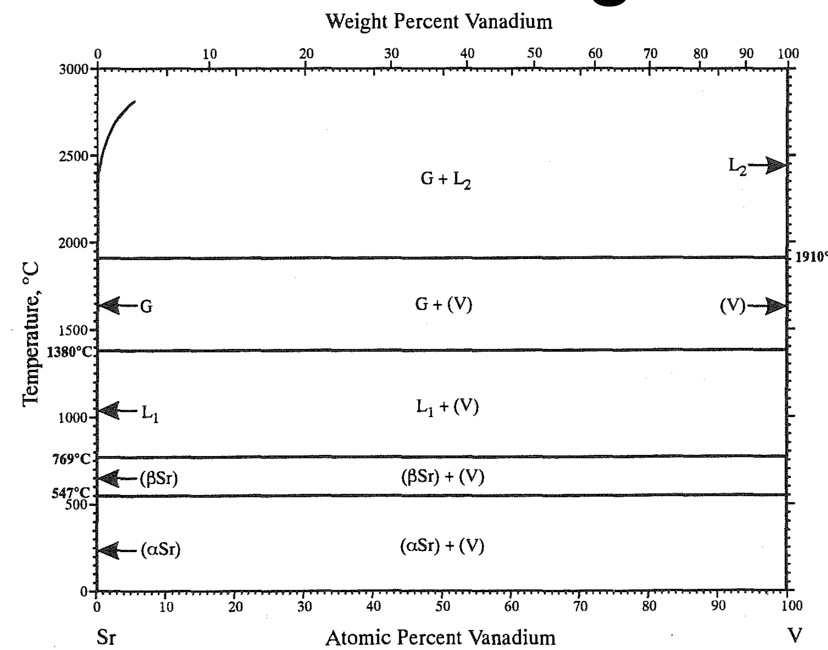

Ti

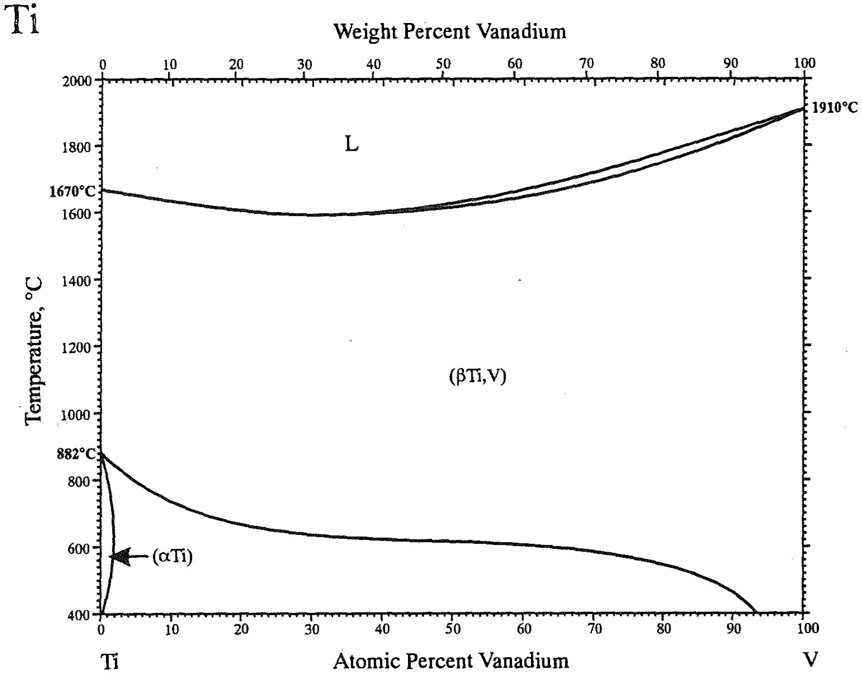

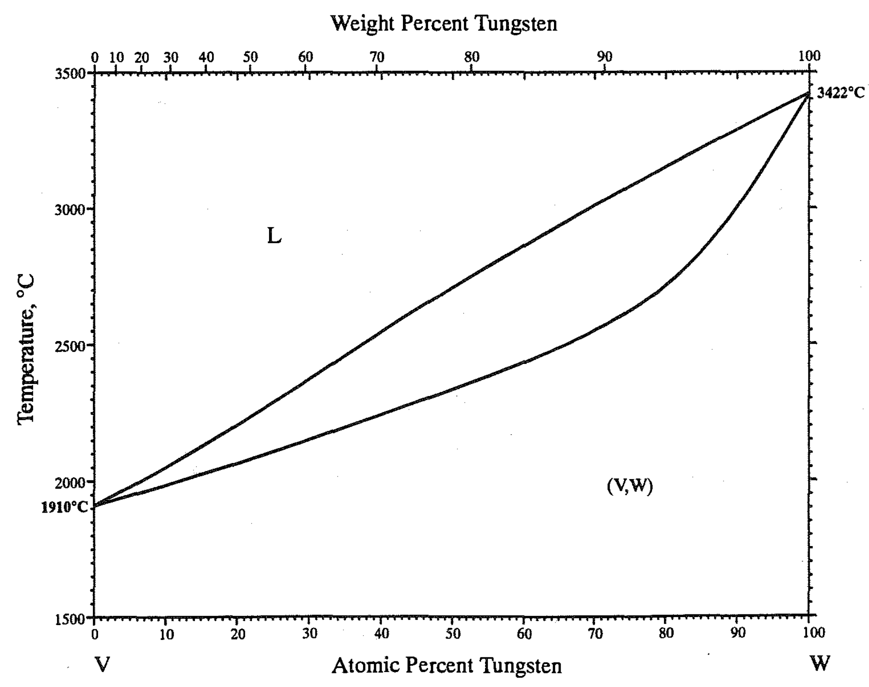

What crucible would you use for V in MBE?

(a) C

(b) Sr

(c) Ti

(d) W